

# Tectonic resurgence of the Mysore plateau and surrounding regions in cratonic Southern India

K. S. Valdiya

Geodynamics Unit, Jawaharlal Nehru Centre for Advanced Scientific Research, Bangalore 560 064, India

The landscape of the Dharwar Craton in the southern part of the Indian Shield is much more dynamic than previously thought. Strike-slip and oblique-slip movements along the NNE/N–SSW/S trending active faults in the eastern part of the Dharwar Craton and along the NNW/N–SSE/S oriented faults in the west gave rise to horst mountains – the Biligirirangan–Mahadeswaramalai in the east and the Sahyadri in the west. Synchronously, the breakup of the NNW–SSE striking linear fault-blocks along the ESE–WNW oriented reverse faults and shear zones was responsible for the peculiar *en echelon* configuration of the high ranges of the Sahyadri and its escarpment, the Western Ghat.

The buckling and breaking of the crust of the Southern Granulite Terrane of South India along E–W oriented reverse faults and shear zones culminated in the emergence of the Nilgiri terrane. Its elevation above 2500 m and the youthful precipitous scarps, across which streams descend as waterfalls through canyons, imply neotectonic movements that overtook the Archaean mobile belt, resulting in the

uplift of the massif and its geomorphic reshaping. Strong fluvial response to inferred active tectonism, coupled with the pattern of seismicity, indicates late Quaternary reactivation of ancient shear zones and faults of the Shield. The neotectonic movements along them are indicated by, among others, the upstream river ponding that gave rise to lakes in the past and is manifest in stagnant bodies of water at present, and the deformation of very young fluvial and lacustrine sediments in the proximity of identified active faults. The various geomorphic features adduced collectively taken in conjunction with the reality of the faulted framework of the terrane that is recurrently shaken by earthquakes testify to active tectonism. The stream ponding associated with deflections is discernible consistently all along the length of the same fault, – even rivers that have large discharges during the monsoon. The time-span of the formation of the palaeolakes implies Late Pleistocene to mid Holocene reactivation of the causative faults. The pattern of epicentral distribution conforming to the trends of faults further supports this deduction.

ONE among the three continental nuclei of the Indian subcontinent<sup>1</sup> the Dharwar Craton (DC) in the southern part of the Indian Shield is described as a stable continental region comprising several Precambrian terranes (Figure 1). Unaffected by compressional tectonics since the  $550 \pm 50$  Ma Pan-African events, the DC has been experiencing slow intermittent uplift ever since Madagascar broke away from this fragment of the East Gondwanaland ~ 90 million years ago, particularly after it collided with Asia in the Palaeocene to Early Eocene time. The uplift and resultant landscape development have been attributed to movements of the epeirogenic<sup>2</sup> or cymatogenic<sup>3,4</sup> tectonism that took place over a long period of time ranging from Late Mesozoic to Holocene, or to the buoyancy of the crust related to hotspots or plumes<sup>5</sup>. The Mysore Plateau of undulating landscape of nearly 800 m elevation is bordered on three sides by rugged mountains that rise more than 1000 to 1800 m above it (Figure 2). While the high tableland drops northward to yet another plateau 700 to 800 m in

altitude, in the south it is sharply separated from the granulite terrane of the Nilgiri massif by an E–W oriented shear zone (Figure 1). Making the western border, the Sahyadri mountain – with many of its peaks rising higher than 1800 m – abruptly ends in more than 700 m high scarps against the undulating coastal belt that is no more than 40 to 120 m above sea level. The Biligirirangan–Mahadeswaramalai (BR–MM) ranges characterized by summits as high as 1755 m in the eastern part of the DC give way through gentler slope-breaks to the Tamil Nadu plains to the east.

Cut by long, deep faults of Precambrian antiquity, the DC is recurrently shaken by earthquakes of small to moderate magnitude. The present study was carried out to find out whether there is any relationship between the development of the Dharwar Craton landforms and the multiplicity of seismogenic faults.

It is commonly believed that the landscape of the Indian Shield in southern India evolved through a slow geomorphic process and attendant changes<sup>3,7–9</sup>. However, (a) the descent as high waterfalls and cascades of old meandering rivers like the Kaveri, Bedti, Sharavati,

e-mail: uday@jncasr.ac.in

Pykara, etc. as they leave the elevated tableland, (b) the canyon courses through the bordering mountain ranges of the rivers and streams that otherwise flow lazily in their wide valleys, and (c) the abrupt rise in the midst of thickly soil-covered flat terrains of the Mysore Plateau and Coastal Belt of the mountains and the linear hills characterized by straight steep planar, practically gullyless scarps exposing remarkably fresh Precambrian rocks, indicate that not much time has elapsed since these features were formed. Well-drained topographic escarpments are known to expose unweathered fresh rocks of any age. However, in the study area the notably rectangular or linear pattern of unweathered fresh rocks conforming to the linear trends of faults and of topographic rises or eminences in sharp contrast to the surrounding areas with thick mantle of lateritic or richly ferruginous soil cannot be taken as a case of normal erosion giving rise to islands of fresh rocks amidst highly weathered rocks covered by thick red soil. Furthermore, it is observed that: (1) the river gradients increase and stream incision becomes considerably pronounced along the margins of the Mysore upland so that the river profiles are marked by convexity, (2) the drainage system displays sharp shifts in river courses along lines coinciding with zones of faulting, (3) the decrease in river gradients upstream of many zones of faulting is manifest in aggradation and even river ponding, and (4) in the western and eastern fringes of the elevated Dharwar Craton, the hills that stand high in the flat terrains are characterized by steep furrowless planar

scarps that form conspicuous fronts or escarpment along the margins of the uplands. These observations, implying relatively recent movements, are at variation with the assumption of a long-term landscape evolution over a protracted geological period ranging from the Late Mesozoic to the Present.

### Geological setting

The Indian Shield in southern India encompasses in its vast expanse (Figure 1) a number of contrasted lithotectonic terranes, each with its distinctive history of development, multiple episodes of diastrophism and several cycles of igneous activity<sup>10-12</sup>. The Dharwar Craton is a product of crustal growth that took place mainly between 3400 and 2500 Ma. It is divided into two parts by a N-S shear zone and the conspicuous belt of ~2500 Ma Closepet Granite (Figure 1). The Eastern Dharwar Craton (EDC) is made up of predominant 2600–2500 Ma granites, gneisses and migmatites, and subordinate schists, quartzites, metabasalt and komatiitic ultrabasic rocks occurring in the middle of the terrane. The Western Dharwar Craton (WDC) comprises predominant migmatites, gneisses, and 3400 to 3000 Ma granites, collectively described as the Peninsular Gneiss, with minor linear enclaves of metamorphosed ultrabasic igneous and pelitic sedimentary rocks. Resting on and associated with the Peninsular Gneiss is the 2900 to 2600 Ma succession of the Dharwar Supergroup, made up of basic and ultrabasic schists with banded iron formation in the lower part, and conglomerate, limestone, greywacke and chert in the upper.

In the south, the DC is severed from the Archaean mobile belt – the Southern Granulite Terrane (Figure 1) – by the E-W trending Moyar–Bhavani Shear Zone (M–BSZ) and Palghat–Kaveri Shear Zone (P–KSZ)<sup>13,14</sup>. Characterized by Pan-African (624–472 Ma) thermal events<sup>15,16</sup>, the M–BSZ is made up of mylonites and ultramylonites<sup>17</sup> resulting from dominantly dip-slip shear movements<sup>18</sup>. South of the Moyar shear zone is the Nilgiri massif that is made up of dominant charnockites and associated granulites and rises to a height more than 2500 m (see Figures 1, 18 and 20).

South of the P–KSZ, the Southern Granulite Terrane is essentially a Late Archaean to Palaeoproterozoic mobile belt. It is characterized by widespread charnockite formation and coeval intrusion of alkali granites and syenites at ~550 Ma and strong signatures of uplift and exhumation.

### Seismicity in Southern Peninsular India

There is no recorded history available of past earthquakes in southern India. One can only infer from the literature mentioning geomorphic developments that

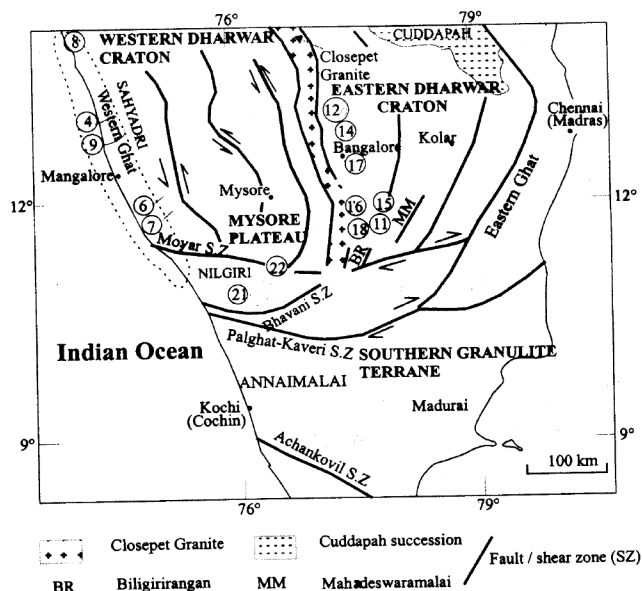


**Figure 1.** Indian shield in southern India, comprising Western Dharwar Craton, Eastern Dharwar Craton and Southern Granulite Terrane, shows the location of the Mysore Plateau flanked in the west by the Sahyadri, in the east by the Biligirirangan–Mahadeswaramalai Hills, and in the southwest by the Nilgiri massif. Encircled numerals locate the areas described in the text.

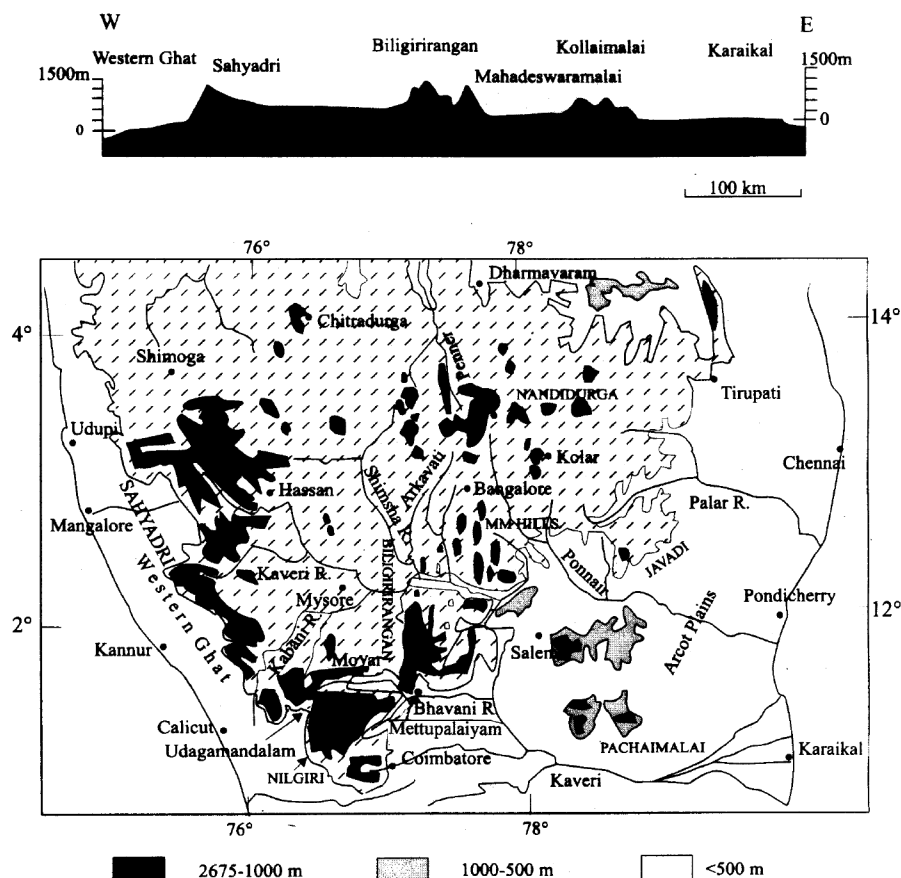


**Figure 2.** Mysore plateau, having an average elevation of nearly 800 m above sea level, is bordered on three sides by high mountains that rise 300 to more than 1000 m above the undulating terrain of the plateau. The profile at the top<sup>6</sup> shows the topographic peculiarity of the Indian Shield in the Dharwar Craton. It should be obvious that the Sahyadri and the Biligirirangan–Mahadeswaramalai Hills stand high like horst mountains. Slanting dashed lines depict Mysore Plateau.

took place suddenly and conspicuously, such as the 1341 event resulting in the emergence of the 14 km by 24 km island of Vaipin near Kochi (Figure 3) and the formation of a lake with attendant devastating flood<sup>20</sup>. The 1507 earthquake at Billankote near Nelamangala (WNW of Bangalore), and the 28 January 1679 earthquake in the Coromandal (Madras) coast find mention in the Tamil literature<sup>21</sup>. The 1784 'strong concussion felt at Cochin'<sup>20</sup>, the ground shaking events of 31 December 1881 and 28 February 1882 at Calicut, of 14 October 1882 in the Allatur–Palghat belt, and of February 1823, September 1841, November 1845, March 1856, August 1856 and September 1856 in the Trivandrum area<sup>22</sup> are manifestations of the seismicity in recent historical times (Table 1). Repeat periods of moderate earthquakes being quite long – longer than the documented earthquake history – it is only through geomorphic data that past movements have been deduced.

Even though the Indian Shield in South India is at present shaken frequently by earthquakes (Table 1 and Figure 3), the recent strain rates determined geodeti-

cally is less than 10 nanostrain/yr (ref. 23), the strain rates per year being  $2.4 \times 10^{-10}$  for the Southern Granulite Terrane,  $3.3 \times 10^{-10}$  for the Moyar–Bhavani Shear Zone and  $4.0 \times 10^{-10}$  for the Dharwar Craton<sup>24</sup>. The magnitude of the earthquakes are usually less than M 5.5 – ranging mostly from M 2 to 4 in the Richter scale<sup>25,26</sup>.

The seismicity is largely (~80%) confined to linear belts<sup>27–29</sup>. The microseismicity possibly represents manifestation of reactivation of fractures and fissures with which the whole terrane is riddled. Significantly, the estimated principal stresses suggest a strike-slip environment over the region 12° to 16°N – the Dharwar Craton – with a dominant NE-trending compression<sup>30</sup>. The 1984 Bangalore earthquake of M 4.6 indicated right-lateral motion<sup>31</sup> or a combination of reverse and strike-slip deformation at the focal depth<sup>30</sup>. The June 1988 earthquake of M 4.5 at Idukki likewise resulted from strikeslip movement (Figure 3 inset). In the northwestern part of the study area, the hypocentre locations of more than 400 earthquakes reveal fragmentation in the seismicity pattern and the seismic segments

**Table 1.** Earthquakes of  $M \geq 4.5$  (in the Richter scale) and earthquake swarms in the Indian Shield south of  $16^\circ\text{N}$ <sup>28,82</sup>

| Date                   | Coordinates   | Location                    | Magnitude (M)/Intensity (MM) |
|------------------------|---------------|-----------------------------|------------------------------|
| 19 October 1800        | 15.60 : 80.10 | Ongole                      | VI                           |
| 10 December 1807       | 13.10 : 80.30 | Madras                      | VI                           |
| 16 September 1816      | 13.10 : 80.30 | Madras                      | VI                           |
| 29 January 1822        | 12.50 : 79.70 | Madras–Nellore              | VI                           |
| 2 March 1823           | 13.00 : 80.00 | Madras                      | VI                           |
| 22 August 1828         | 13.00 : 75.00 | Malabar                     | VII (5.7)                    |
| 12 March 1829          | 13.00 : 75.50 | Bangalore                   | 5.8                          |
| 1 April 1843           | 15.20 : 76.90 | Bellary                     | VII (5.7)                    |
| 23 August 1858         | 11.40 : 76.00 | Malabar                     | VI                           |
| 3 January 1859         | 12.50 : 79.00 | North Arcot                 | VI                           |
| 24 June 1865           | 18.80 : 76.80 | Coimbatore                  | IV                           |
| 1 September 1869       | 14.50 : 80.00 | Nellore                     | VI                           |
| 12 August 1889         | 13.10 : 80.30 | Madras                      | VI                           |
| 28 February 1900       | 10.80 : 76.80 | Coimbatore                  | VII (5.8)                    |
| 27 April 1901          | 12.00 : 75.00 | North of Calicut            | VI                           |
| 7 January 1916         | 13.00 : 75.50 | Bangalore                   | VI                           |
| April–June 1952        | 11.00 : 78.00 | Rangamalai                  | V–VI                         |
| Later 1952–Early 1953  | 10.00 : 76.80 | SW of Madurai               | V                            |
| 26 July 1953           | 9.90 : 76.30  | Cochin                      | VI                           |
| 12 October 1959        | 15.70 : 80.10 | Ongole                      | VI                           |
| 13 October 1959        | 15.60 : 80.10 | Ongole                      | VI                           |
| September 1961         | 11.40 : 75.70 | Calicut                     | IV                           |
| 20–21 January 1965     | 13.50 : 77.50 | Kolar                       | IV                           |
| March–June 1966        | 13.00 : 80.20 | Tambaram                    | IV                           |
| October–December       |               |                             |                              |
| 27 March 1967          | 15.60 : 80.10 | Ongole                      | 5.4                          |
| January 1971–May 1972  | 12.60 : 76.90 | Mandya                      | V                            |
| 16–17 May 1972         | 12.40 : 77.00 | Mandya                      | 4.2–4.6                      |
| 29 June 1972           | 10.80 : 76.80 | Coimbatore                  | VI                           |
| 12 May 1975            | 13.80 : 75.30 | North of Shimoga            | 5.6                          |
| November–December 1980 | 15.30 : 76.30 | Hospet                      | IV                           |
| 20 March 1984          | 12.70 : 77.80 | SE of Bangalore             | 4.5                          |
| 20 May 1984            | 12.69 : 77.82 | Nelamangala                 | 4.6                          |
| 27 November 1984       | 12.87 : 78.00 | Tirupattur                  | 4.5                          |
| 3 December 1987        | 15.50 : 80.21 | Ongole                      | 4.5                          |
| 7 June 1988            | 9.82 : 77.22  | Idukki                      | 4.5                          |
| 3 May 1990             | 13.00 : 75.50 | North Bangalore             | 4.6                          |
| 14 November 1993       | 12.20 : 77.05 | Malavalli (S. of Bangalore) | 4.5                          |

have close links with the Western Ghat escarpment that trends NNW–SSE, and with the WNW–ESE shear zone along which the Warna river flows<sup>32</sup>. The seismicity pattern thus points to the DC tectonic boundaries being active.

The Dharwar Craton (DC) is characterized by clearly recognizable fold axes and NNW–SSE trending faults and fractures (Figures 4 and 10) which change to N/NNE–S/SSW in the northern and northeastern parts<sup>10,29,33,34</sup>. Less prominent are the E/ESE–W/WWN oriented reverse faults laterally becoming shear zones. The northerly faults are not very straight or continuous but show stepovers, giving rise to a overstepping trend, particularly in the western margin of the Mysore upland. One of the NNW–SSE trending faults – characterized by mylonite and shear zone and traceable from the SE of Mysore to the NNE of Chitradurga – defines the lithotectonic boundary between the EDC and the WDC<sup>35,36</sup>, bearing impress of both strike-slip and

dip-slip motions of the Precambrian times<sup>10,37</sup>. Deep seismic refraction studies confirm the existence of the fault that caused uplift of the Eastern Dharwar Craton relative to the WDC<sup>38</sup>.

Cut as it is by the NNW–SSE trending strike-slip and oblique-slip faults, the Dharwar Craton exhibits geomorphic rejuvenation and peculiar drainage and anomalous river responses to neotectonic movements<sup>2,3,7–9,29,39–47</sup>.

## The Sahyadri and Western Ghat Escarpment

### *En Echelon ranges and faults*

Forming the western mountainous part of the DC, the Sahyadri (Figures 1 and 2) encompasses the NNW–SSE trending *en echelon* ranges that abruptly end as steep slope-breaks at their northwestern ends and as very high



scarps that face west. It has been described as an example of a retreating rift-flank. Also, it is difficult to subscribe to the notion that flexural-isostatic adjustment is responsible for the escarpment retreat. For, the Western Ghat escarpment is not straight or curved as presumed, but characterized by *en echelon* pattern of slope-breaks and scarps as already stated. A slow escarpment retreat cannot explain this. The mountainous terrane is cut by a multiplicity of predominant NNW-SSE trending *en echelon* sinistral faults and less common ESE/E-WNW/W oriented shear zones (Figure 4). It may be reiterated that both the mountain ranges and the escarpment are delimited by faults, and both have *en echelon* configuration. The elevation of the peaks of the outer (western) ranges reaching as much as 1931, 1892, 1715, 1598 and 1355 m (see Figures 4 and 9) – which is considerably more than the general ground level of  $800 \pm 100$  m of the soil-covered Mysore Plateau – implies differential uplift of the fault-delimited blocks.

West of the more-than-700 m high escarpment lies the Coastal Belt of an undulating terrain, characterized

by low ridges and shallow depressions that have approximately NNW-SSE trend and by a thick mantle of laterite. The elevation of this erosion surface (coastal belt) varies from 40 to 120 m above sea level. Lithologically and structurally the Coastal Belt is not different from the mountainous Sahyadri. However, the altitudinal contrast is very great and the change of elevation is quite abrupt.

Interestingly, the geological, geomorphological and tide-gauge data near Mangalore on the coast ( $13^\circ\text{N}$ ) confirm earlier studies that this coastal tract has been rising at the rate of  $1.95 \pm 0.14$  mm/yr and  $3.22 \pm 1.1$  mm/yr relative to the areas, respectively to the north and the south<sup>48–50</sup>. Significantly, these three areas (of observation) lie on three different NNW-SSE trending fault-delimited low ridges (see Figures 4 and 9). It may therefore be inferred that these three linear blocks have different rates of uplift. This can happen only if the faults that delimit them are active to different degrees. The current rates of uplift indicated by tide-gauge data ( $= 3$  mm/yr) and spirit-level data ( $= 6$  mm/yr) are higher than the Quaternary rates and are consistent with the recent strain ( $< 10$  nanostrain/yr) measured geodetically in southern India<sup>50</sup>.

There is no surface evidence for the existence of a continuous coast-parallel inland 'West Coast Fault' that has been recognized on the basis of sharp gravity gradients and spectacular slope-breaks<sup>4,51–54</sup>. It is noteworthy that the rate of sediment deposition in the offshore continental margin is very low<sup>55,56</sup>. The development of the Western Ghat escarpment cannot therefore be attributed solely to the erosion that is believed to have caused slow scarp retreat<sup>3,7,8,57,58</sup>. It may be pointed out that the escarpment shows *en echelon* offsetting of slope breaks – and not straight or curved pattern if the cause were just the slope retreat.

### Offshore continental margin

Like the Sahyadri and the Coastal Belt, the offshore continental margin is also cut by the NNW-SSE oriented *en echelon* faults and fractures and by ESE-WNW trending shear zones, the former delineating gentle ridges and shallow depressions. Off the Karnataka coast, the NNW-SSE trending 40–60 m deep grabens, a mid-shelf ridge, a shelf-margin basin<sup>59</sup> and a series of 5 to 10 m high reefal ridges<sup>60</sup> demonstrate near similarity of the structural trend and architecture and the topographic layout of the inland coastal belt with those of the offshore continental margin. Significantly, the submarine features are offset by ESE/E-WNW/W oriented faults<sup>59</sup>. They extend inland (eastwards), sinistraly offset the shoreline and palaeobeaches<sup>42,46</sup> and cause rivers like the Bedti to drop as high waterfalls.

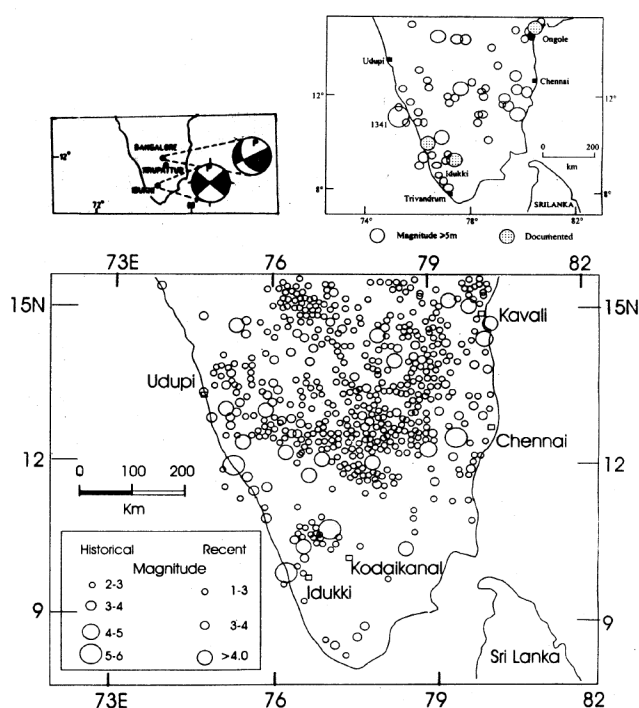


**Figure 3.** Distribution of small and moderate earthquakes (magnitude in Richter scale)<sup>26</sup> in the Indian Shield in southern India. Comparison with Figures 4, 10 and 20 would make it quite obvious that the earthquakes are more frequent in the regions cut by the multiplicity of faults. The map shows not only the natural seismicity but also rock bursts which might have triggered microseismicity in the nearby fractures and shear zones. Hence the picture of diffuse seismicity. The left inset provides the available fault-plane solutions of two events<sup>31</sup>. The right inset shows important moderate earthquakes in South India<sup>82</sup>. The magnitude of earthquakes given in the Richter scale.

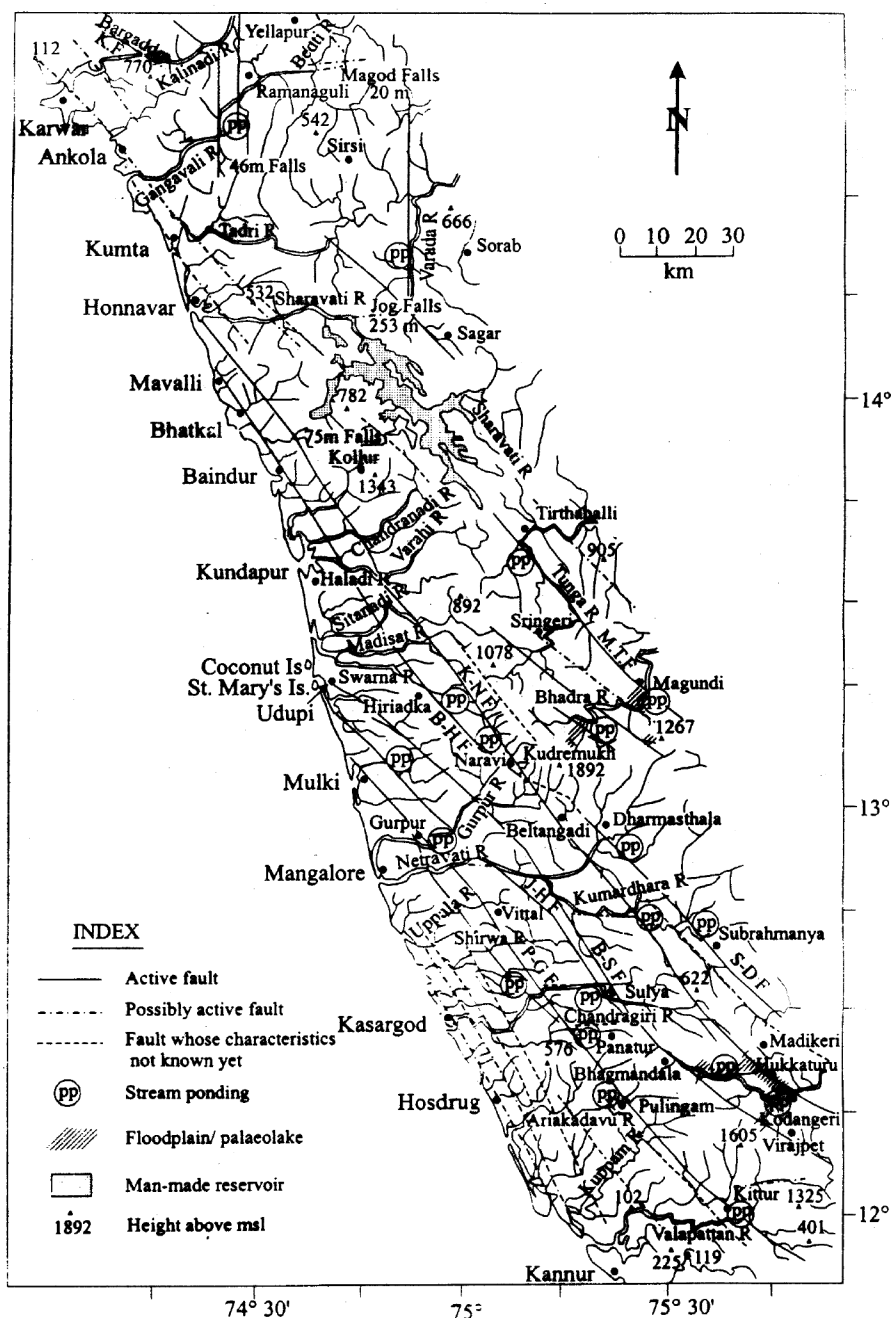


**Figure 4.** Sahyadri and coastal domains of the Western Dharwar Craton are cut by dominant NNW–SSE trending faults and ESE/E–WNW/W-oriented reverse faults that laterally become shear zones. Note the deflection and bending of rivers as they cross the faults. The locations of palaeolakes and stream ponding upstream of the faults are noteworthy. (MTF, Magundi–Tirthahalli Fault, SDF, Subrahmanya–Dharmasthala Fault, KNF, Kodangeri–Naravi Fault, BHF, Bhatkal–Hiriadka Fault, BSF, Bhagamandala–Sulya Fault, PGF, Pulingam–Gurpur Fault). Faults that caused river ponding in the past and the present are designated as ‘active faults’. The ‘possibly active faults’ are those that are associated with fluvial aggradation and have caused pronounced deflection of rivers and streams.

## Stream behaviour

### Bedrock incision

All rivers and streams that flow west and descend across the western margin of the Mysore Plateau have

cut deep V-shaped valleys. The abrupt drop as waterfalls through gorges and descent as cascades of the rivers that flow unhurriedly in their upper reaches on the 700–900 m high Sahyadri domain indicate that not much time has elapsed since the formation of the scarps. The river beds show convex profiles (Figure 5)

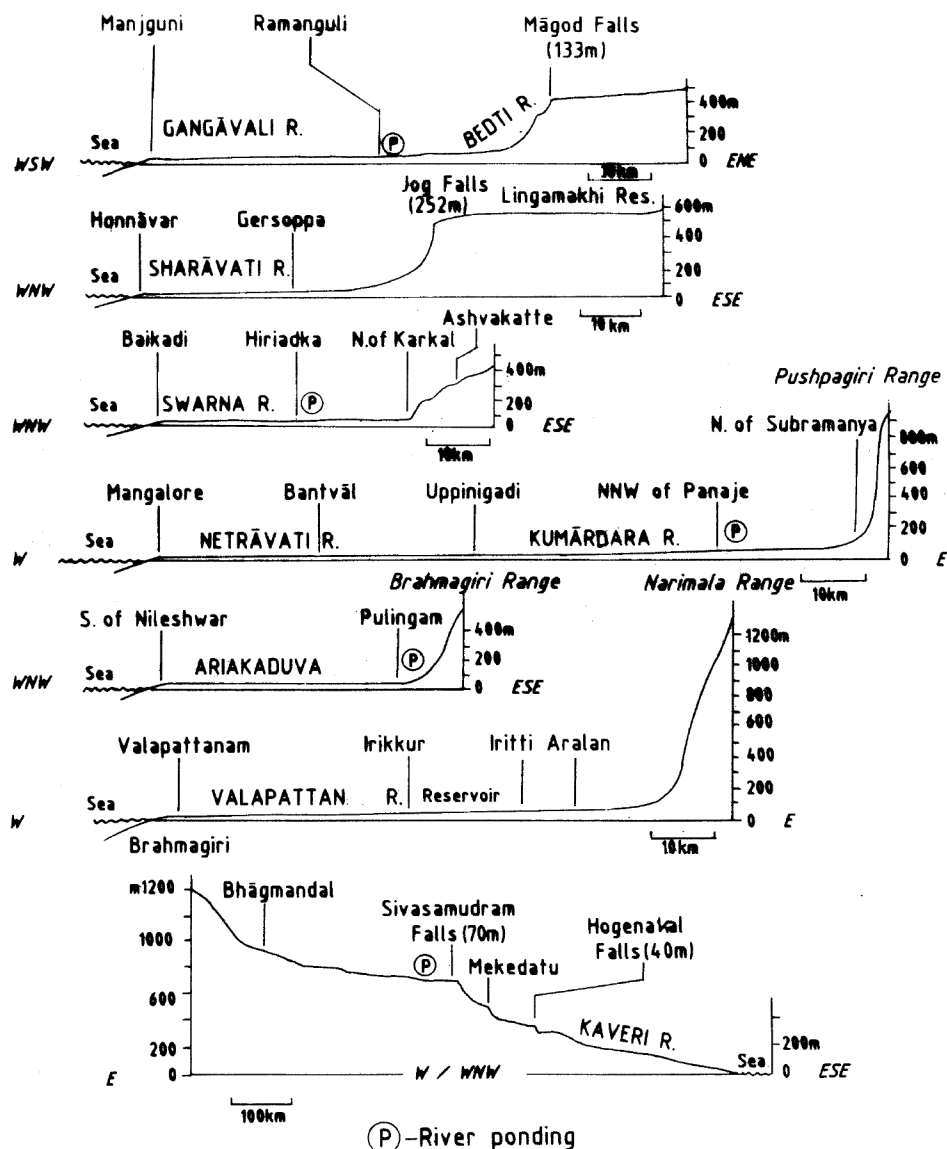


**Figure 5.** Topographic profiles of the beds of the rivers that cross the faulted terrains in the Dharwar Craton. Note the gentler gradient of the west-flowing streams (first six profiles) in the coastal belt where ponding is very common upstream of these faults, and the convexity of the profiles in the narrow 'Ghat' reach of the rivers.

in their narrow Western Ghat reaches. In this 'Ghat' segment of the valleys, the straths are covered with a thin veneer of gravelly detritus commonly less than a metre above the river bed. In the low-elevation undulating coastal belt, where most of the channels have the gradients varying from  $1^{\circ}$  to  $1.5^{\circ}$  (Table 2), the channels are flanked by gravelly terraces, which are not very thick and therefore get flooded during heavy discharges. Consequently, the terraces have cappings of overbank fine sands, silts and muds. The rivers have cut into bed-rocks and the terraces are covered by overbank sediments. There is a perceptible-to-conspicuous decrease in their gradients as they cross the NNW–SSE trending

faults. The decrease of the river gradient, interpreted as due to the uplift of the downstream block, both in the lowland and the highland, is generally manifest in a number of ways: (1) Aggradation in the upstream reach where dumping of bed loads gives rise to bars that the flow must pass around so that the channels are widened<sup>61</sup>; (2) Increased aggradation leading to decrease in channel-bed depth, reduced carrying capacity and increased flood frequency with attendant overbank fine sediments and in some places development of swamps and even lakes where damming is complete<sup>62–64</sup>; (3) Rivers display anastomosing pattern or increase in the sinuosity of meandering in the upstream stretches<sup>61,62</sup>;

**Table 2.** Deflection and ponding of streams that cross faults in the Dharwar Craton

| River                   | Locality          | Mean elevation<br>above sea level (m) | Direction of<br>deflection | Amount of<br>deflection | River<br>gradient |
|-------------------------|-------------------|---------------------------------------|----------------------------|-------------------------|-------------------|
| Gangavali               | Ramanguli         | 50                                    | N5°E–S5°W                  | 83°–110°                | ~ 2°              |
| Bhatkal                 | Mudbhatkal        | 10                                    | N34°W–S34°E                | 115°                    | ~ 1.5°            |
| Swarna                  | Near Hiriadka     | 15                                    | N30°W–S30°E                | 100°                    | ~ 1.5°            |
| Shirwahole (Udayavara)  | Sura              | 10                                    | N47°W–S47°E                | 75°                     | ~ 1.5°            |
| Mulki                   | Damaskatte        | 15                                    | N17°W–S17°E                | 74°                     | ~ 1.5°            |
| Gurpur                  | Polali            | 10                                    | N45°W–S45°E                | 85°                     |                   |
| Kumaradhara (Netravati) | Near Panaje       | 70                                    | N37°W–S37°E                | 114°                    | 1°                |
| Payaswini               | Sulya             | 95                                    | N17°W–S17°E                | 112°                    | 1°                |
|                         | Paichar           | 75                                    | N20°W–S20°E                | 70°                     | 1°                |
| Ariakaduva              | Pulingam          | 50                                    | N40°W–S40°E                | 82°                     | ~ 1.5°            |
| Kaveri (upper reaches)  | Kodangeri         | 855                                   | N42°W–S42°E                | 77°                     | ~ 3°              |
| Bhadra (upper reaches)  | Kalasa            | 760                                   | N56°W–S56°E                | 25°                     | ~ 1.5°            |
| Tunga (upper reaches)   | Near Thirthahalli | 595                                   | N45°W–S45°E                | 77°                     | ~ 1°              |
| Hemavati                | Mavinakere        | 840                                   | N10°W–S10°E                | 80°                     | ~ 2.5°            |
| Shimsha                 | Iggaturu          | 615                                   | N3°E–S3°W                  | 90°                     | 1°                |
| Kaveri                  | Talakad           | 633                                   | N15°E–S10°W                | 75°                     | ~ 2.5°            |
| (Middle reaches)        | Kollegal          | 625                                   | N10°E–S10°W                | 110°                    | ~ 2.5°            |

(4) Increased degradation in the channels across uplifted blocks in an attempt by the rivers to re-establish their gradient in the face of river-profile deformation<sup>61</sup>. It is noteworthy that practically all these features are observed in the river valleys in the coastal belt below the Western Ghat, implying active tectonism.

In addition to these features, several nearby streams and rivers deflect conspicuously the same way all along the extents of the faults as they cross the NNW–SSE and N–S trending faults (Figure 4 and Table 2). Locally they exhibit loops or hairpin geometry (see Figures 6 and 8). Obviously the bending of streams indicates control of faults on the drainage. There is no denying that the deflection of streams was guided by erodable rocks of the fault zone. However, the development of conspicuous loops implies strike-slip movements concurrent with the flow in the valleys of the meandering streams. Furthermore, the past ponding (represented by palaeolake deposits) and the continuing obstruction to flow (represented by stagnant bodies of water over long reaches) by the *same* fault cannot but be interpreted as implying activeness of the fault. It can therefore be surmised that the abrupt deflections of streams and the formation of conspicuous loops in the channels were due to the activeness of the faults.

### Stream ponding

It is noticed that each of the dozen faults of regional extent has not only consistently caused conspicuous deflection of the streams, but also their discernible ponding where it crosses them all through its extent. Not only the main rivers, but also the tributary

streams – even quite minor ones – evince upstream stagnation of water at the fault crossings. In other words, every fault is associated, all along its strike, with stream deflection and causes stagnation of water as it crosses the valleys. The narrow passages the streams/rivers have cut through the downstream blocks bear eloquent testimony of entrenchment.

The Magundi–Tirthahalli Fault (M–TF in Figures 4, 6 *d*, 7 *c* and 8) has caused ponding of the Bhadra River at Magundi and of the Tunga River and its tributary Malati SW and W of Tirthahalli. The Kodangeri–Naravi Fault (K–NF) is likewise responsible for the upstream stagnation of the Kaveri at Kodangeri (Figure 7 *b*), the Kumaradhara and its tributaries near Panaje (Figure 7 *a*), the Kela and Swarna branches near Naravi, and the Haladi River near the township Haladi. This fault is marked by a 75-m waterfall in the Calkin Bare Hill near Bhatkal (Figures 4 and 8). The Bhatkal–Hiriadka Fault (B–HF) has caused blockage in the Mudbhatkal stream near Bhatkal, in the Swarna near Hiriadka (east of Udupi) and in the Kela near Naravi. The Kaveri near Bhagamandala (Figures 4 and 8), the Payaswini near Sulya (Figure 6 *b*) and the Udayavara at Sura (about 10–15 km west of Karkal) have been ponded upstream of the Bhagamandala–Sulya Fault (B–ST). The Jalsur–Damaskatte Fault (J–DF) is associated with the impoundments in the Mulki River near Damaskatte and in the Payaswini near Jalsur. The Pulingam–Gurpur Fault (P–GF) is responsible for the anomalously excessive sand accumulation in the Gurpur River near Polali, and the ponding of the Shirwa near Perla, the Chandragiri branches near Panatur, the Ariakaduva branches at Pulingam (Figure 6 *c*) and the Valapatan River near Iritti (Figures 4 to 8).

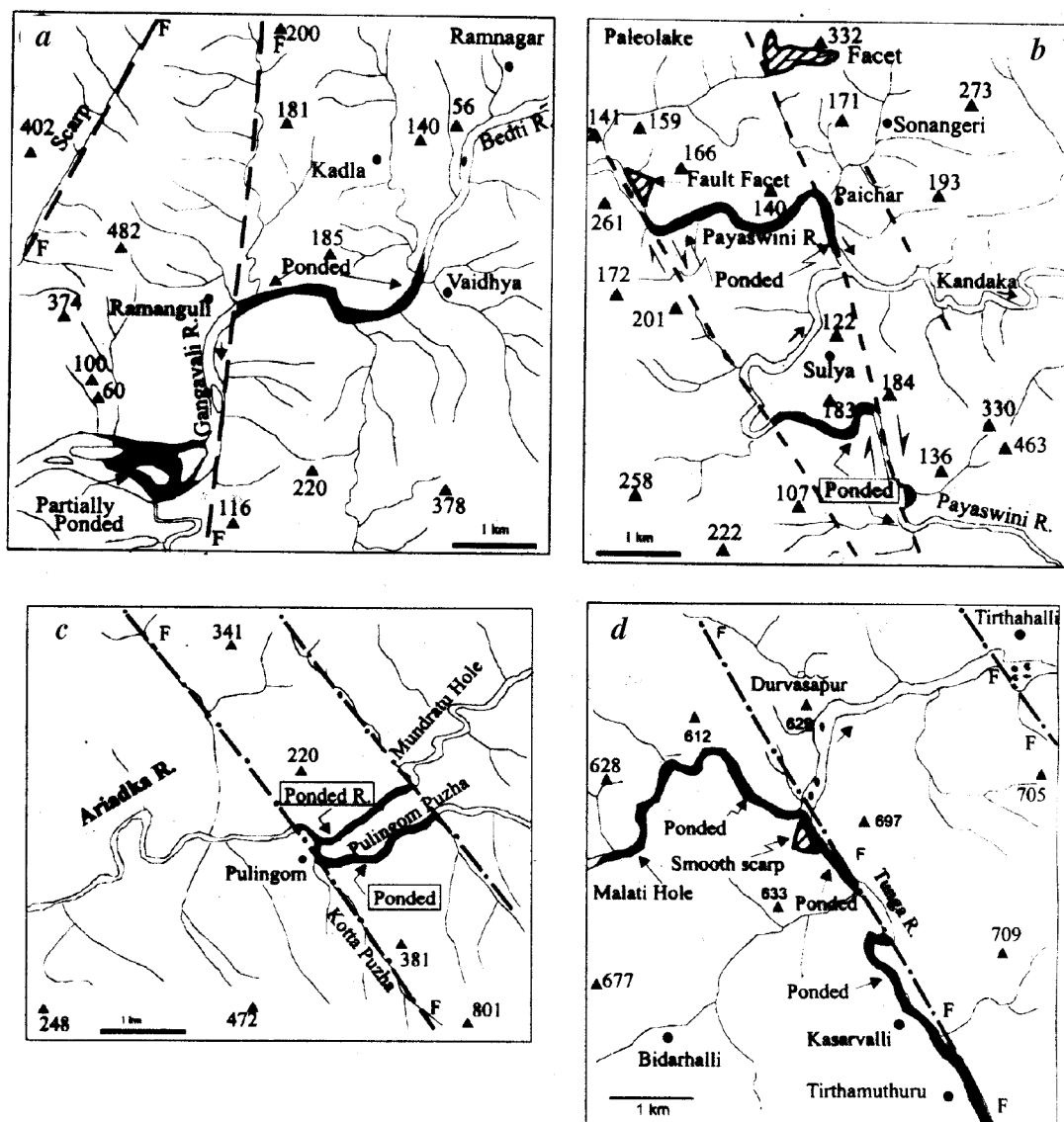


**Figure 6.** Rivers deflect conspicuously as they cross the NNW–SSE to N–S trending faults. Locally they exhibit hairpin geometry or development of loops. (For locations, please see Figure 8). *a*, Gangavali River is ponded east of Ramanguli on the Ankola–Yellapur road (area ③ in Figure 1); *b*, Payaswini is stagnant between two active faults in the Sulya area on the Mangalore–Madikeri road (area ⑥ in Figure 1); *c*, Two branches of the Ariakaduva River in northern Kerala are ponded (area ⑦ in Figure 1); *d*, SW of Tirthahalli in the Sahyadri domain both the Tunga and its tributary Malati Hole are ponded (area ⑨ in Figure 1).

The ponding of the Gangavali at Ramanguli and Hosakambe (Figure 6*a*) and the Varada east of Sidapur (Figure 4) are other examples of present-day river ponding upstream of the NNW/N–SSE/S trending faults.

In the tectonically resurgent Mysore Plateau, rivers carrying sediments during floods year after year would have filled the pools had these been formed as a result of differential resistance of rocks to river-bed erosion. In the monolithic terrane – characterized by monotony of rocks like granite-gneiss and charnockite-granulite –

the differential resistance hypothesis cannot explain the development of prolonged impoundments. Moreover, the pools are not seen where schists, amphibolite and other relatively softer rocks are intercalated with gneiss or charnockites. Rather, they are located where the faults cross the valleys.

Interestingly, in the Konkan Coast immediately to the north of the study area the Kapashi River that follows one of the NNW–SSE-trending lineaments is characterized by (i) a narrow straight course, (ii) flat terraces on the eastern side, and many 10–15 m high waterfalls on

the western side, and (iii) natural ponding created by E–W blocks<sup>65</sup>.

### Evolution of Sahyadri and its scarp face

The youthfulness of the fault scarps of the Sahyadri Ranges and of the Coastal Belt ridges, the anomalous behaviour of streams (such as the abrupt deflection, the hairpin geometry of the drainage) (Table 2 and Figures 4, 6 and 8), the cutting of incisions across raised ridges

within the coastal plain, the repeated ponding of rivers as they cross the NNW–SSE trending faults, and the intimate association of palaeolakes (Figure 4) with these faults provide compelling evidence for the neotectonic resurgence that has overwhelmed the western part of the Dharwar Craton, particularly the Sahyadri domain. Considered in conjunction with other evidence, the meandering rivers that flow in their wide valleys with very gentle slopes and then through progressively deepening valleys or gorges before dropping as high waterfalls across faultline scarps, cannot be attributed to passive escarpment retreat.

It seems that while the fault-defined blocks of the Coastal Belt failed to rise beyond 40 to 120 m above sea level, the NNW–SSE trending fault blocks of the Sahyadri domain rose up 700 m to more than 1800 m to give rise to the mountain ranges, the heights of which vary from block to block. The change in elevation is quite abrupt and the contrast of topographic relief is very great.

Isostatic uplift following profound erosion cannot explain this spectacular geomorphic contrast between the lithologically and structurally identical Coastal Belt and the Sahyadri domain. The great heights of the Sahyadri can therefore be attributed only to the neotectonic resurgence. And the neotectonic movements are related to the reactivation of the NNW–SSE trending faults.

Following the pronounced oblique-slip displacement along the very active NNW–SSE trending faults, the linear blocks of the Western Dharwar Craton when pushed northwards broke due to frictional resistance along the ESE/E–WNW/W oriented southwardly inclined reverse faults and shear zones. The northwestern edges of these broken linear fault blocks eventually became steep slope-breaks and their western fault-delimited sides formed spectacular scarps (Figure 9). In all probability, the stronger and greater northerly push or advance of the eastern blocks due to strike-slip displacement, coupled with the considerable uplift of the Sahyadri, is responsible for the peculiar morphology and pattern of the Western Ghat. The elevation of the faulted blocks diminishes progressively northwards – from 2695 m in the Cardamom Hills in Kerala to 2620 m in the Nilgiri massif to 1892 m in the Kudremukh Range and finally to 810 m in the Sira–Talaguppa Range (see Figures 9 and 20). One of the plausible explanations for this is that there was a steadily northward-decreasing uplift due presumably to northward tilting of the fault blocks. The northerly tilt may be attributed to the pronounced faulting or thrusting up of the Southern Granulite Terrane (SGT) on the approximately E–W trending shear zones – the M–BSZ and P–KSZ (Figures 1 and 2), the impact of thrusting diminishing northwards.

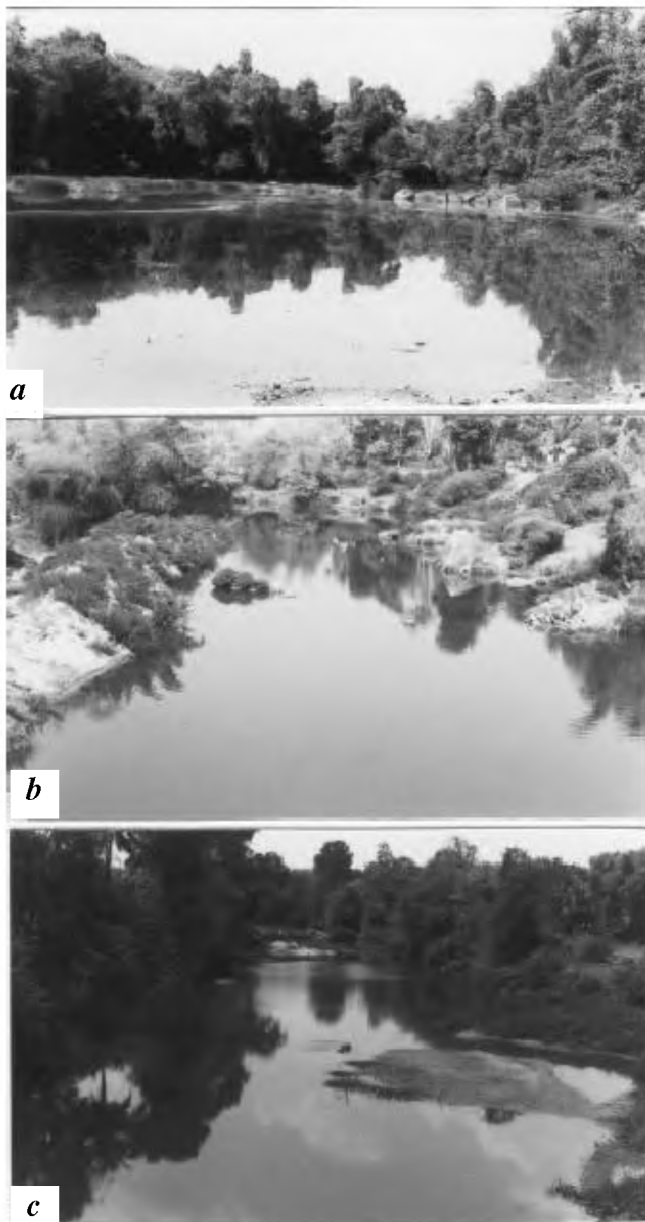


**Figure 7.** Ponded rivers upstream of active faults that are responsible for their blockade. (Locations of areas shown in Figure 8). *a*, Kumaradhara, 3 km NNW of Panaje on the Mangalore–Subrahmanya road (area ⑥ in Figure 1); *b*, Kaveri at Kodangeri, 15 km SE of Madikeri (area ⑦ in Figure 1); *c*, Bhadra near Magundi in the Kudremukh area (area ⑧ in Figure 1).

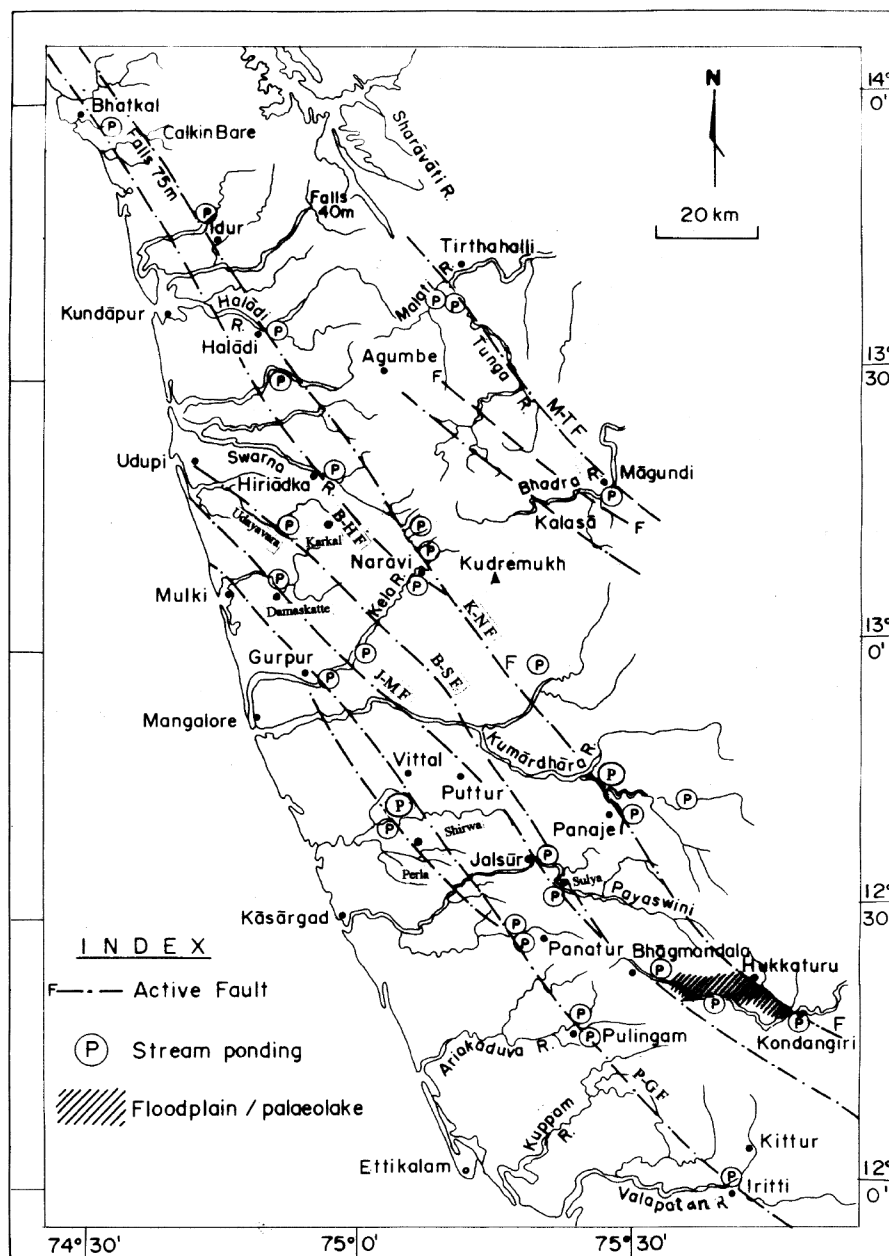
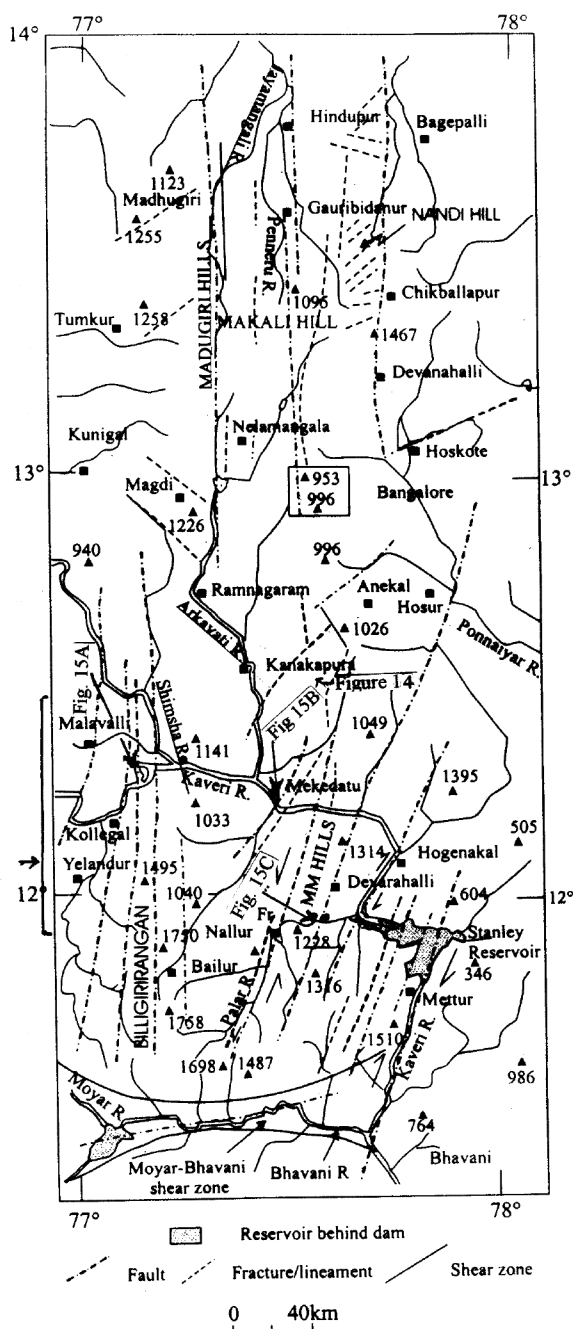


**Figure 8.** Simplified map showing only those active faults which are associated with drainage deflection, palaeolakes and stream ponding – those that have been discussed in the text.

### Emergence of BR-MM Hills and their extensions

Forming the eastern fringe of the Mysore Plateau and rising abruptly 700 to 900 m above the nearly 800 m undulating surface of this tableland (Figures 1 and 2), the Biligirirangan-Mahadeswaramalai (BR-MM) Hills constitute a high linear barrier across the southeasterly-flowing Kaveri River (Figures 2 and 10). The top of these hills have an undulating landscape (Figure 11a) characterized by capping of red lateritic soil and by the streams that flow unhurriedly in their winding courses,

locally breaking into marshes or lakelets and then dropping down the steep scarps of the mountain ranges. The west-facing flanks are very steep to near vertical scarps (Figure 11b), which expose remarkably fresh charnockite and granulites of Precambrian to Pan-African ages. These straight planar scarps, devoid of or with only a few straight furrows, demarcate the N-S trending faults that longitudinally cut the terrane of the BR-MM Hills<sup>29</sup>. It is quite evident that the BR-MM domain is a horst mountain that took shape in the late Quaternary along the eastern borders of the Mysore Plateau.





change. The initiation and acceleration of gully erosion in the fault zone are attributed to tectonic activity on the faults that delimit the elevated linear ridges<sup>29</sup>. This is further borne out by stream ponding in the fault-crossed valleys such as seen at a number of places south of Bangalore – in the Arkavati valley at Manchenabele, in the Rayatmala valley at Vaddarakuppe and in the Antargange stream at Uchchivalase discussed in the following section.

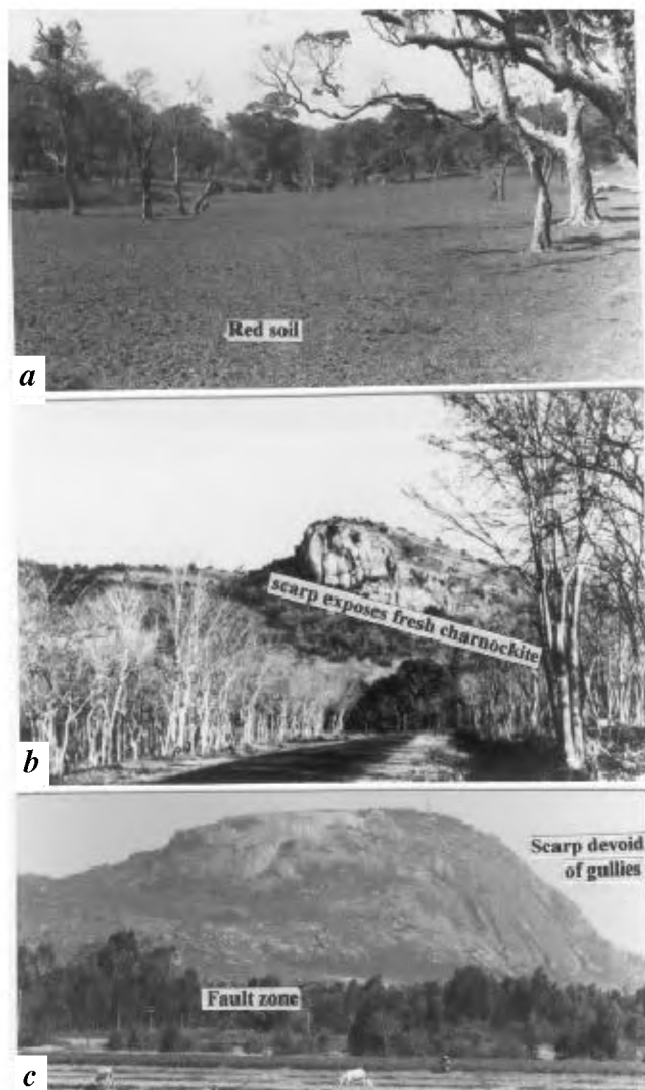


**Figure 11.** *a*, Top of the Biligirirangan Hills is characterized by gently undulating terrain underlain by laterite and red soil. It represents a planation surface, now at an elevation of roughly 1400 m above sea level and more than 900 m above the Mysore surface that is characterized by the same geomorphic features and similar soil mantle (area 18 in Figure 1); *b*, High scarps, locally vertical and exposing remarkably fresh Precambrian rocks form the west-facing slope of the BR Hills. A N–S fault demarcates the limit of this scarp (area 18 in Figure 1); *c*, NandiDurga Hill abruptly rising 300–400 m above the soil-covered Bangalore planation surface (~ 900 m), has steep to nearly vertical planar scarp remarkably devoid of gullies. A N–S trending fault at the foot of the hill is characterized by a belt of mylonites (area 14 in Figure 1).

### Ponding of the Kaveri and its tributaries

Upstream (west) of the fault line demarcating the border of the Biligirirangan Hills, the valley of the Kaveri (Figure 13) is characterized by an approximately 10 m thick succession of black clay, obviously deposited in a standing body of water<sup>67</sup>. The deposits of black clay abruptly end against the N–S trending Kollegal Fault and form remarkably flat stretches of uniform elevation in the otherwise undulating terrain of the Mysore

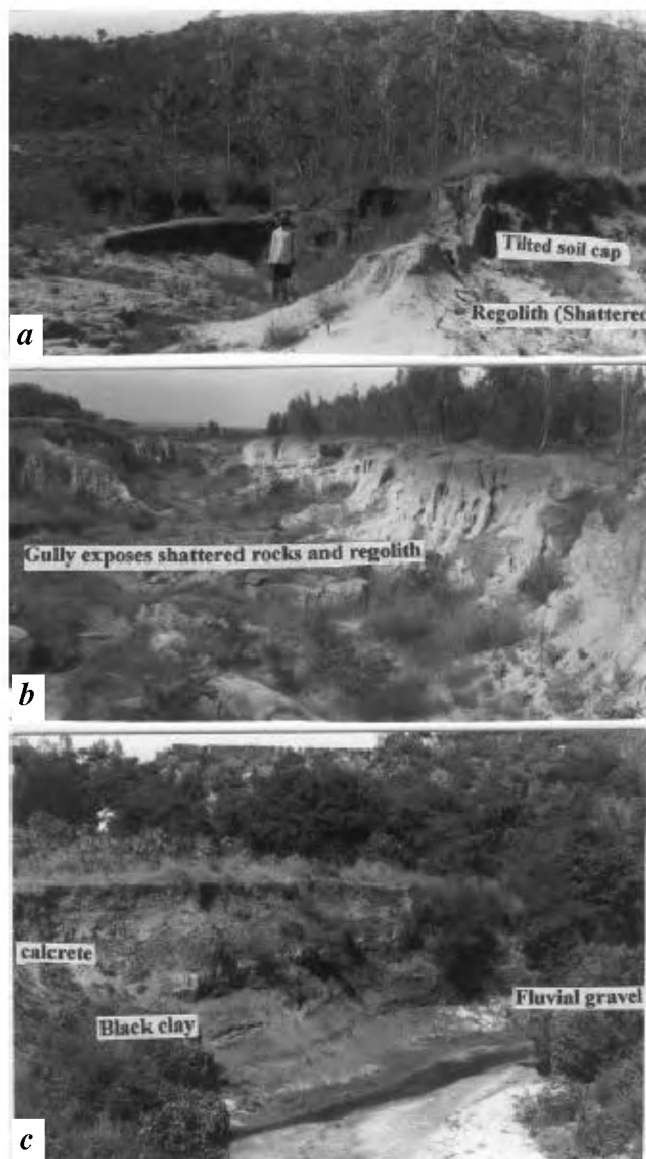


**Figure 12.** *a*, Westward tilted regolith with red soil capping along the faulted foothill of the NandiDurga Hill shown in Figure 11 *c*. The fault trends in the N–S direction (area 14 in Figure 1); *b*, Severe gully erosion and consequent ravineland development is very conspicuous in the fault zone at the foot of the fault-defined NandiDurga Hill and elsewhere (area 12 in Figure 1); *c*, Palaeolake succession in the Rayatmala stream at Vaddarakuppe, SSE of Bangalore. The Rayatmala is a petty tributary of the Arkavati River (see Figure 10). The fluvial gravel at the base is succeeded by black clay characterized by carbonate concretions (area 17 in Figure 1).

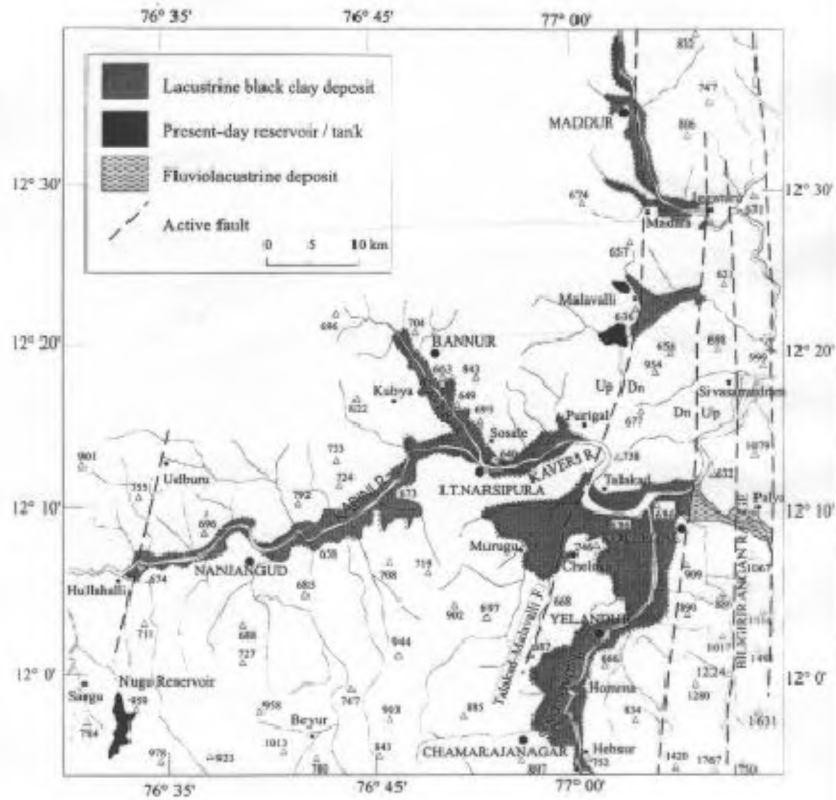


**Figure 13.** Represented by a 5–7 m thick accumulation of black clays, the palaeolakes in the Kaveri Basin provide very fertile lands for paddy and sugarcane cultivation. The lacustrine sediments abruptly end against the N–S trending Kollegal–Iggaturu Fault. Note that this fault juxtaposes the lacustrine sediments against fluvial sediments east of the fault. Later faulting along the Talakad–Malavalli Fault resulted in slight westerly tilt and in elevation difference of the lake sediments (area ① in Figure 1).

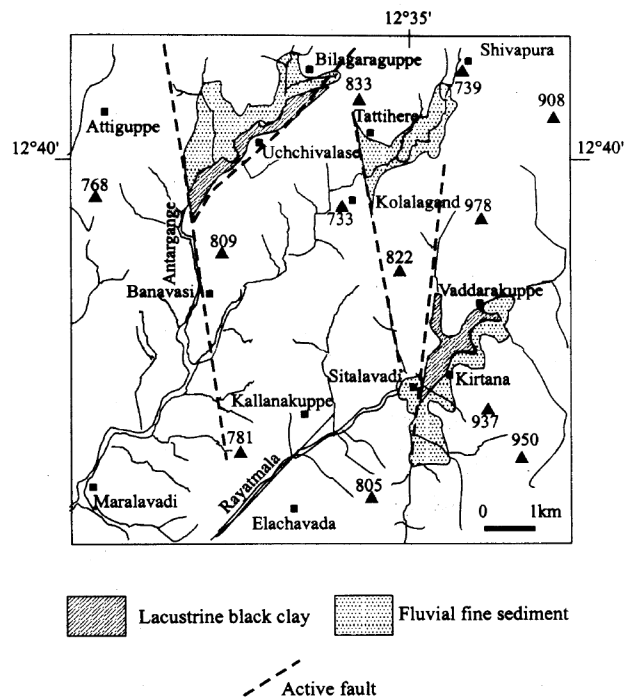


**Figure 14.** Movements along the NE–SW and N–S trending faults caused ponding of the streams Antargange and Rayatmala in the eastern part of the basin of the Arkavati River, a tributary of the Kaveri (see Figure 10). The resultant lakes are represented by 7 to 13 m thick accumulations of black clay in the area SSE of Bangalore. The lacustrine clay succeeds the fluvial gravel and is intimately associated with calcareous nodules including rhizocretions in the upper part (area ② in Figure 1).

Plateau. The sharp linear juxtaposition of the ~ 26,000-year old 6 to 10 m thick black clay-succession against the Precambrian rocks and the limit of the clay deposits coinciding with the fault line is to be seen in the context of the lacustrine clay deposits extending only upstream

of the fault crossing and not occurring anywhere downstream. These facts imply that the development of the impediments to stream flows was due to the uplift on the delimiting fault. The fact that the same fault throughout its extent caused perceptible to pronounced stream ponding in a number of places goes to show that the fault is active. The example is the Kollegal Fault, upstream of which not only the Kaveri and its tributary Suvarnavati but also the Shimsha and its tributary streams were ponded (Figure 13).

These are now intensively used for paddy and sugar-cane cropping. The clays transitionally overlie fluvial gravel and sand in the channels or are resting directly on the weathered country rocks in wide valley flanks. Closer to the channels, finer sediments brought by recurrent floods cover the black clay as overbank alluvial sediments. Likewise at the foot of the uplifted BR Hills in the east, eroded material brought by hill torrents conceal the lacustrine black clay. The palaeolakes stretch quite far upstream<sup>67</sup> – 38 km in the Suvarnavati upto ESE of Chamarajanagar, 52 km in the Kabini upto west of Nanjangud, 45 km in the Kaveri upto NW of T. Narasipura, 10 km in the Hul Halla upto Malavalli, and 29 km in the Shimsha upto north of Maddur (Figure 13)

Invariably associated with and sharply delimited by the N–S trending Kollegal Fault that defines the BR Hills, the palaeolakes (formed upstream of the delimiting fault) in the Kaveri Basin (Figure 13) thus provide the most compelling evidence for neotectonic displacements along the faults. The ages of the sediments (Table 3) at the base in these lakes constrain the time of reactivation of the causative faults that cross the rivers. In a number of localities, the deformation of Recent sediments is seen in the proximity of identified active

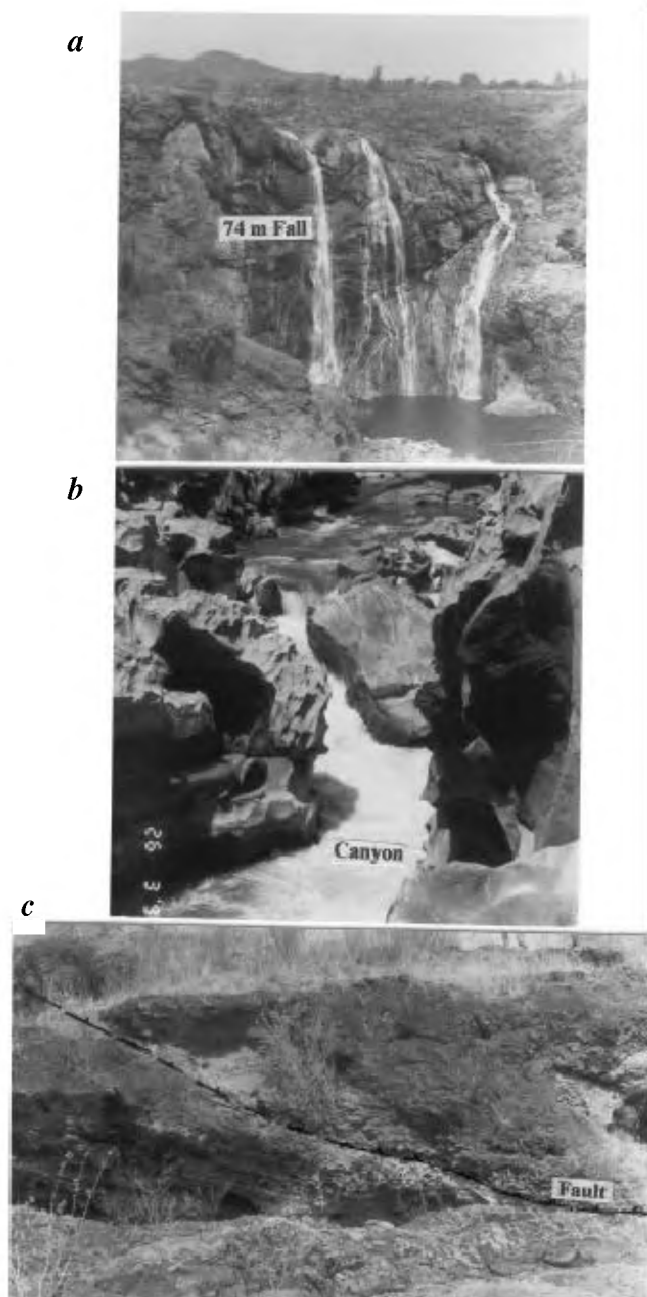


**Figure 15.** *a*, Before entering the gorge cut through the BR–MM mountain barrier, the northward-deflected Kaveri drops 78 and 70 m across the active faults at Sivasamudram, south of Bangalore (area ⑩ in Figure 1); *b*, Kaveri gorge becomes a chasm, so narrow that ‘a goat can leap across it’ at Mekedatu (Mekedatu = goat leap) where an active fault crosses the valley (area ⑮ in Figure 1); *c*, Carbonate-encrusted Pleistocene fluvial gravel terrace in the Palar rivulet (west of the Stanley Reservoir) is deformed and partly overthrust in the proximity of an active NNE–SSW trending fault in the southern part of the MM Hills (area ⑪ in Figure 1).

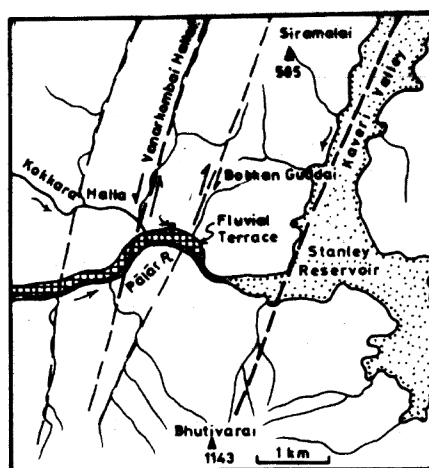


**Figure 16.** Lower reaches of the Palar is cut by NNE–SSW trending faults, about 4 km west of the Stanley Reservoir in the Kaveri basin. Very young gravel-made terraces (square pattern) lining the banks of the Palar are deformed due to movement along the faults (area ⑪ in Figure 1).

# SPECIAL SECTION: SCIENCE IN THE THIRD WORLD

**Table 3.**  $^{14}\text{C}$ -ages of sediment succession of individual palaeolakes in the Kaveri Basin in the Mysore Plateau and of the Nilgiri Hills in the Southern Granulite Terrane (Dating done by G. Rajagopalan at Birbal Sahni Institute of Palaeobotany, Lucknow)

| Region           | River/stream basin                                  | Location of palaeolake          | Sample position below surface <sup>†</sup> (m) | Measured age (T½-5730 ± 40 yr) (yr BP) | Calibrated age range* (yr BP) |
|------------------|---|---------------------------------|--|--|-------------------------------|
| SSE of Bangalore | Antargange <sup>67</sup><br>Rayatmala <sup>67</sup> | Uchchivalase<br>Vaddarakuppe    | 7.0  | 26470 ± 990                            | Beyond dataset                |
|                  |   |                                 | 0.90   | 14290 ± 280                            | 17530–16730                   |
|                  |   |                                 | 4.25   | 18740 ± 320                            | 22760–21750                   |
|                  |   |                                 | 5.25   | 20150 ± 320                            | 24360–23340                   |
|                  |   |                                 | 6.25   | 21850 ± 320                            | Beyond dataset                |
|                  |   |                                 | 7.25   | 25030 ± 1740                           | Beyond dataset                |
| SSW of Bangalore | Arkavati <sup>67</sup><br>Hemavati <sup>68</sup>    | Manchenabele<br>Mosalehosahalli | 8.25   | 25490 ± 1560                           | Beyond dataset                |
|                  |   |                                 | 0.40   | 1870 ± 180                             | 2000–1570                     |
|                  |   |                                 | 0.25   | 1770 ± 110                             | 1820–1540                     |
|                  |   |                                 | 0.65   | 1900 ± 90                              | 1950–1710                     |
| Kollegal         | Kaveri <sup>67</sup><br>Suvarnavati <sup>67</sup>   | Chalukavadi<br>Muguru<br>Homma  | 2.35   | 4310 ± 190                             | 5280–4580                     |
|                  |   |                                 | 0.10   | 4470 ± 110                             | 5290–4860                     |
|                  |   |                                 | 0.25   | 8290 ± 140                             | 9470–9030                     |
|                  |   |                                 | 0.20   | 3540 ± 170                             | 4090–3590                     |
| Nilgiri          | Moyar <sup>74</sup>                                 | Sandyanalla-I                   | 1.40   | 7850 ± 140                             | 8980–8440                     |
|                  |   |                                 | 1.50–1.55                                      | 2230 ± 130                             | 2350–2060                     |
|                  |   |                                 | 1.60–1.65                                      | 2550 ± 90                              | 2750–2470                     |
|                  |   |                                 | 1.70–1.75                                      | 3040 ± 50                              | 3340–3160                     |
|                  |   |                                 | 1.80–1.85                                      | 4050 ± 110                             | 4810–4410                     |
|                  |   |                                 | 1.90–1.95                                      | 4680 ± 120                             | 5590–5300                     |
|                  |   | Sandyanalla-II                  | 2.30–2.40                                      | 8680 ± 140                             | 9910–9530                     |
|                  |   |                                 | 0.62–0.64                                      | 3730 ± 100                             | 4080–3740                     |
|                  |   |                                 | 1.21–1.24                                      | 28150 ± 2180                           | Beyond acds                   |
|                  |   |                                 | 1.59–1.62                                      | 31790 ± 1180                           | Beyond acds                   |
|                  |   |                                 | 1.80–1.83                                      | 39690 ± 2700                           | Beyond acds                   |
|                  |   | Pykara <sup>74</sup>            | 0.7–1.0  | 5600 ± 120                             | 6500–6290                     |
|                  |   |                                 | 1.2–1.5  | 7760 ± 140                             | 8680–8410                     |
|                  |   |                                 | 1.7–2.0  | 10620 ± 180                            | 12910–12350                   |
|                  |   |                                 | 2.2–2.5  | 14480 ± 240                            | 17720–16980                   |
|                  | Kundah <sup>74</sup>                                | Nanjanad<br>Colgrain-I          | 2.0–3.0  | 4130 ± 100                             | 4700–4800                     |
|                  |   |                                 | 0.2–0.5  | 7580 ± 130                             | 8450–8210                     |
|                  | Bhavani <sup>74</sup>                               | Upper Bhvani                    | 0.7–1.0  | 17140 ± 200                            | 20800–20020                   |
|                  |   |                                 | 0.2–0.4  | 1980 ± 100                             | 2040–1820                     |
|                  |   |                                 | 1.3–1.5  | 5860 ± 150                             | 6850–6490                     |
|                  |   |                                 | 2.0–2.3  | 19100 ± 300                            | 23170–22170                   |

\*Using Calib Ver 4.12 (Radiocarbon age calibration programme of the University of Washington, USA). (acds, age calibration data set).

<sup>†</sup>For each palaeolake, the dates refer to different levels of the single lake succession. The samples were collected by different groups of workers, with different objectives.

faults, particularly where they rest upon strongly sheared rocks. The deformation is doubtless due to neo-tectonism.

The ponding of the Rayatmala and Antargange tributaries of the Arkavati River (Figures 2, 10 and 14) is represented by a 7–10 m thick accumulation of lacustrine clay with fluvial sand and silt. The base and top of the black clay of the palaeolake at Vaddarakuppe (Figure 12c) and Uchchivalase (Figure 14) give dates of ~ 26,000 and 14,000 yr BP, respectively<sup>67</sup>, implying Late Quaternary movements along the causative faults. Presumably, the Kollegal Fault responsible for the Kaveri Basin lakes was reactivated nearly in the same period. Far to the west-northwest, the Mosalehosahalli palaeolake in the Hemavati valley SE of Hassan (Figure 2) existed from about 14000 yr BP to nearly 1300 yr BP

(ref. 68). In other words, the lakes of the larger Kaveri basin embracing Hemavati, Shimsha, Arkavati, Kaveri, Kabini and Suvarnavati valleys are penecontemporaneous. The Kaveri-valley lakes must have lasted until about 4900 to 5300 yr BP as indicated by the ages of top layers of the lake sediment at Muguru and Chelukavadi (Figure 13).

Interestingly, the lacustrine sediments in the Shimsha and Kaveri valleys have been vertically cut by the Talakad–Malavalli Fault (Figure 13). The altimetric difference of the lake deposit on the two sides of the fault is 10 m. The sediment to the west of the fault is tilted 1–2° westwards. Likewise the alluvial sediment on the western bank of the Kaveri near Talakad is at a higher level than on the eastern bank. Further south, the altitudinal difference of the clay deposit west of

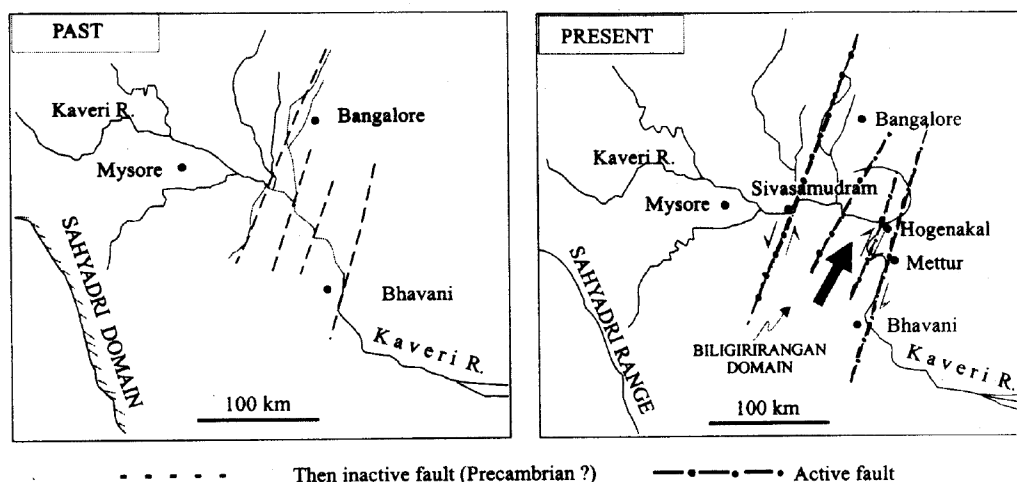


**Figure 17.** The Kaveri abruptly swerves first northwards and then southwards, indicating the controlling influence of the faults. This speculative diagram explains the northward shift of the Kaveri from its original southeasterly course, and its ponding where displacement along faults caused a blockage. Greater and more frequent movements along the easterly faults account for larger cumulative displacement in the eastern side.

Tagarapura (Chelukavadi) is of the order of 5 m, increasing further west at Muguru to 15 m. This implies Late Holocene movement along this fault.

Ongoing movements are indicated by present-day stream ponding in some segments of the fault valleys.

## Deflection of the Kaveri

The lithology of the Dharwar Craton *in the study area* is characterized by preponderant gneisses and granites with very subordinate schists and quartzites. The lithology does not exercise any control on the pattern and deviation of the drainage. Rivers and streams flow across rock assemblages without changing their directions. It is the faults and fractures – particularly those that delimit the terranes – that have profound influence on the drainage pattern.

The eastward-flowing Kaveri abruptly turns first northwards along the Kollegal and Sivasamudram faults and then southwards along the Hogenakal and Mettur faults, the river following the weak fault zones (Figures 2, 10 and 13). These faults define the BR–MM terrane – a horst mountain. The straight steep slopes of these hill ranges, as already pointed out, are characterized by the furrowless planar scarps and the triangular facets that are devoid of gullies. The meandering streams of the mountain terrain drop down these high scarps. These scarps expose fresh rocks of Precambrian ages. The Kaveri that flows sluggishly eastward in its very wide valley in the Mysore tableland abruptly deflects north along the faults (Figures 10 and 13), then drops successively 78, 70, 56, 23 and 40 m (Figure 15 a), and rushes through a narrow entrenched gorge cut across the moun-

tain barrier. The valley has become a chasm (Figure 15 b) where it crosses the active N–S striking fault at Makedatu. The chasm is so narrow that 'a goat can leap across it' (Makedatu = goat leap). The east-flowing (southern) Palar River, just west of the Stanley Reservoir, is crossed by three NNE–SSW trending faults (Figure 16). Paralleling the major Mettur and Hogenakal faults, these faults cut the granulite-facies gneisses and charnockites. The northern bank of the wide Palar is lined by terraces of carbonate-encrusted gravel of Pleistocene age. The gravel bed is tilted, folded and thrust due to compression arising from the movements on the NNE–SSW trending faults – faults that are responsible for landslides in the MM Hills to the north. Folding and faulting of the Pleistocene gravel terrace (Figures 15 c and 16) in the proximity of the NNE–SSW trending faults corroborates the activeness of the faults of the BR–MM domain.

Further upstream, flowing north in the straight fault valley (see Figure 10) the Palar forms a spectacular loop near Nallur. The loop must have been formed as a result of the very slow northward movement of the fault block along the active fault, concurrent with the flow of the river which persisted in keeping its channel open<sup>29</sup>. Presumably, very similar phenomenon affected the Kaveri also, but for a much longer period. Slow, persistent lateral movements along the many faults that longitudinally dissect and delimit the BR–MM domain possibly caused the northward deflection of the river from its original southeasterly course (Figure 17). Taken in conjunction with the neotectonic uplift of the BR–MM Hills, the deflection of the Kaveri must have been due to the fault reactivation in the strike-slip mode. It seems that even as the fault blocks moved

northward and concurrently rose up differentially, the Kaveri persisted in flowing through its original channel. The deeply entrenched easterly course of the Kaveri between faults testify to the uplift of the terrain of this reach. The strike-slip displacements were presumably more frequent and/or stronger eastward<sup>47</sup> as the larger cumulative amount of displacements suggests.

This speculative model on the Kaveri behaviour is at variance with the postulations of Raiverman<sup>69</sup>, Vaidyanadhan<sup>9</sup> and Radhakrishna<sup>3</sup> who believe that the Kaveri earlier flowed ENE through the wide channel of the Northern Palar River in the northeast (different from the Palar that flows past Nallur in the study area) and later swerved abruptly southward at Hogenakal due to its capture by a branch of the Bhavani River. However, the absence of abandoned channels and other fluvial features in the Hosur–Dharmapuri tract SE of Bangalore

(Figure 2) between the Northern Palar Valley and the present course of the Kaveri does not lend support to this postulation.

Significantly, there is an 80-to-90-km northward sinistral shift of the transition zone of the granulite-amphibolite facies along a N–S fault that delimits the WDC<sup>11,70,71</sup>. Quite a part of the 80 to 90 km northward shifting of the Granulite-Amphibolite Facies Boundary must have occurred prior to the Quaternary resurgence. However, in context of the conspicuous sinistral shift of the Kaveri valley – which is quite entrenched in its easterly course – this shift indicates that the movements must have taken place along the faults delimiting the BR–MM Hills, quite after the Kaveri had established its drainage. Admittedly, this horizontal displacement must have taken place over a long geological period beginning at the time when India collided with Asia and must have continued through the later Quaternary.

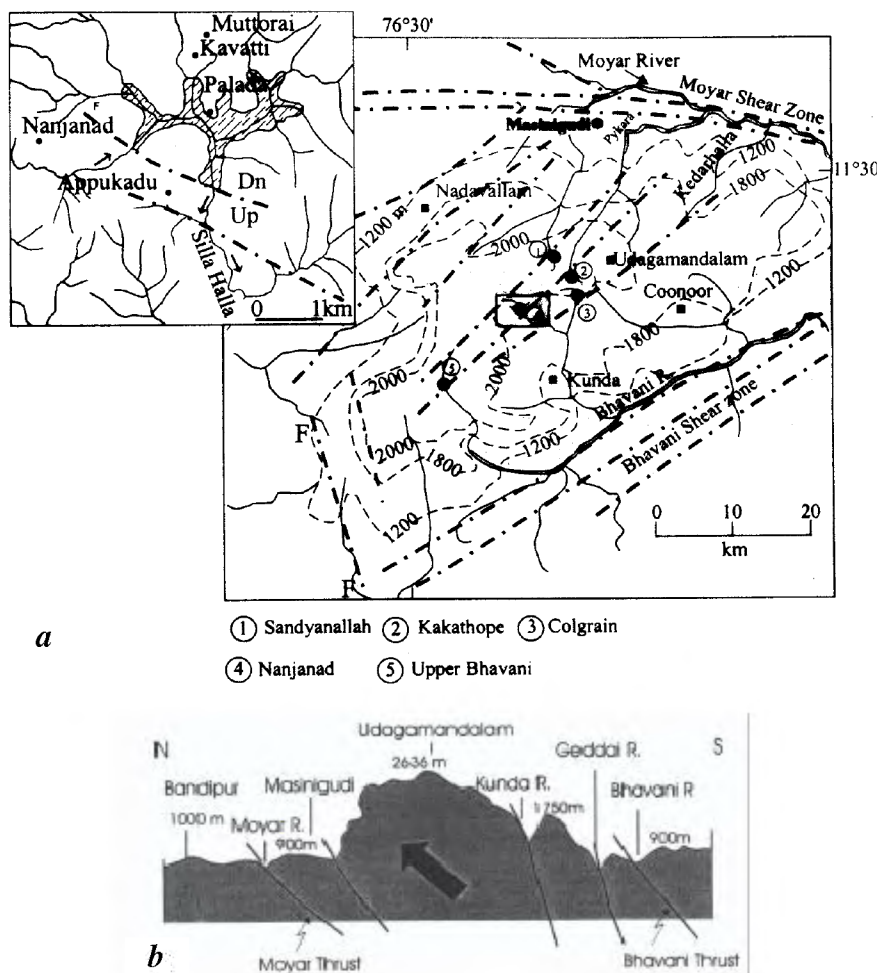


**Figure 18.** *a*, In the fault-dissected Nilgiri massif, streams were ponded, giving rise to lakelets. Location of these palaeolakes are after ref. 74. Inset shows one of these palaeolakes – the Nanjanad–Palada palaeolake (see Figure 19 *c*) formed upstream of the fault paralleling the southern scarp of the massif; *b*, Uplift due to tectonic extrusion of the Nilgiri massif between active reverse faults of the Moyar–Bhavani Shear Zone is responsible for the great height (> 2500 m) of the granulite rocks of deep-seated origin and for the pronounced geomorphic rejuvenation of the terrain<sup>29</sup>.



### E–W shear zones and evolution of the Nilgiri

Southwest of the Mysore Plateau across the Moyar–Bhavani Shear Zone (M–BSZ) lie the lofty Nilgiri Hills (see Figures 1, 2, 18 and 20). Lithologically the Nilgiri is the southerly continuation of the Sahyadri. The E–W trending shear zones are occupied by the Moyar and Bhavani rivers. A number of geomorphic and structural



**Figure 19.** Evidence for Recent movements. *a*, Recent silt is mildly folded close to an active fault in the Moyar–Bhavani Shear Zone (along which the River Bhavani flows) east of Mettupalaiyam (area 22 in Figure 1); *b*, Bhavani River is ponded upstream of an active fault east of Mettupalaiyam (area 22 in Figure 1); *c*, Stream ponding upstream of an active fault gave rise to a flat stretch of lacustrine clay in the Palada–Nanjanad area in the mountain top, south of Udagamandalam (see Figure 18 inset) (area 21 in Figure 1).

developments merit consideration. First, the Moyar and Bhavani rivers have cut their own deposits and are incised deep into the underlying bedrock. Second, the faulted belt of the M–BSZ, immediately south of the Moyar River in the Masinigudi area (Figure 18), is characterized by arching up of rocks, as reflected in (a) the stream ponding, (b) the formation of canyon courses in the otherwise windingly flowing streams like the Pykara and Kedara Halla and then (c) their dropping tens of metres (as much as 86 and 78 m) down into the Moyar. Third, the straight more-than-60-m deep defile of the Moyar River is characterized by largely planar, sparsely furrowed slopes indicating their youthfulness. Fourth, the deformation of recent fluvial sediments (Figure 19 *a*) and ponding of the Bhavani River east of Mettupalaiyam (Figure 19 *b*) indicate neotectonic activity. Fifth, the present-day low level of seismicity in this belt (Figure 4) implying on-going movements in the M–BSZ<sup>29</sup>.

The top of the more-than-2100-m high Nilgiri massif is characterized by a 30 to 40 m thick mantle of laterite and red soils, and a gentle topography with wide valleys of swinging streams. The Nilgiri massif is cut by faults trending NNW–SSE, NE–SW and ESE/E/ENE–WNW/W/WSW<sup>29,72,73</sup>. The high massif is defined on three sides by very steep to practically vertical – even convex – scarps having sheer drops of the order of 1800 to 2000 m. These high scarps expose remarkably fresh charnockites and granulites of the Late Archaean ages in this *tropical land*. Draining the massif, the slow-flowing streams drop through spectacular canyons and chasms as waterfalls or as unbroken cascades. In the massif top there are flat stretches (Figures 18 *inset*, and 19 *c*) of lacustrine deposits comprising silt, black and grey clays with peat. The clay deposits are invariably located upstream of the fault-crossings representing stream ponding due to fault reactivation.

The recalibrated ages of the peat samples near or at the base (Table 3) vary from > 40,000 yr BP to 5,000 yr BP; while the top is dated between 6,500 and 2,000 yr BP (refs 74, 75). It is obvious that the palaeolakes originated in the Late Pleistocene and persisted until about the middle-to-late Holocene period. These palaeolakes are broadly contemporaneous with the palaeolakes in the Kaveri Basin within the Mysore Plateau (Figure 13, Table 3). The analysis of pollens and  $\delta^{13}\text{C}$  values of peats of the palaeolakes of the Nilgiri Hills indicates that it was only in the Holocene time (9000–8000 yr BP) that wetter condition prevailed<sup>75</sup>. Prior to that the climate throughout the Indian subcontinent was considerably arid. It became warm and wet over the Karwar coast and the Arabian Sea as southwest monsoon intensified 10500 to 10000 yr BP and reached its peak 6000–5000 yr BP (refs 76, 77). The climate became dry and hot once again after 4000–3500 yr BP. It will be apparent that the lakes of the Mysore Plateau and Nilgiri Hills originated during the prolonged period of the Late

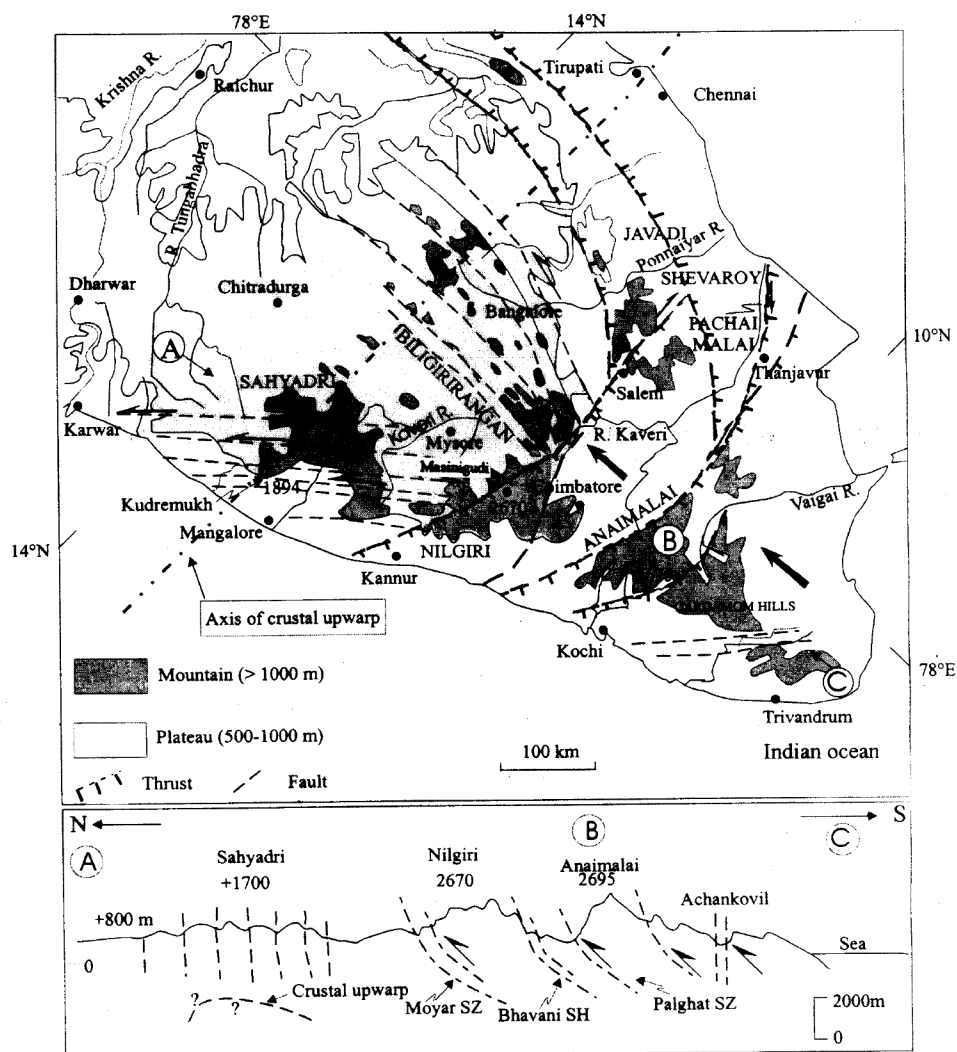


**Figure 20.** Overstressed crust of the Indian Shield in southern India broke along the reactivated reverse faults of the E-W trending Palghat-Kaveri and Moyar-Bhavani Shear Zones of Precambrian antiquity. The southern part (Southern Granulite Terrane) was thrust up as high mountains, culminating eventually in the emergence of the Nilgiri and the Anaimalai-Cardamom Hills. The northward directed thrust movement was transferred partially as strike-slip displacement along the reactivated N-S trending tear faults of the Dharwar Craton, thus giving rise to the two horst mountains on its margins, the Biligirirangan-Mahadeswaramalai Hills in the east and the Sahyadri Mountain in the west.

Quaternary dryness – quite before the beginning of the wet spell. Admittedly, more discharges during wetter spells of climate (~ 30 ka, 18–20 ka, 14 ka) must have brought large quantities of sediments and deposited them in the low-gradient reaches of rivers. The deposition under this environment should have been characterized by intercalation of clays with silts, sands and gravels. However, in the case of palaeolakes described, it was only the clay (6 to 10 m) along with organic matter that was deposited. This must have happened in the standing bodies of water – in which water that stood still for long spells of time. The existence of standing bodies of water in the regime of flowing water implies development of natural dams across the valleys.

## Conclusion

The Indian crust has been under compression ever since India collided with Asia. The ocean floor south of the subcontinent of India – the latter with a stress field in the direction N14°W<sup>27</sup> – is characterized by a series of east-west oriented buckles, attributed to northerly compressional stresses generated by this collision<sup>50</sup>. The recent detection of mid-crustal low-velocity, low-density layers in the Western Ghat and in the Southern Granulite Terrane<sup>78</sup> allows invoking of the buckling of the Indian crust under compressive stresses. The arching up of the Indian Shield in South India along the Mangalore-Madras axis (13°N) points



to this phenomenon, indicating Quaternary neotectonism<sup>48,49</sup>.

The Southern Granulite Terrane encompassing Tamil Nadu and Kerala has an anomalously thicker crust – 4 to 5 km thicker than that of the Dharwar Craton<sup>79</sup>. It is but natural that the northward drifting continental crust under strong compression should have buckled and broken up along the zone of sudden change of the crustal thickness. The E–W oriented shear zones of Precambrian antiquity, characterized as they are by anastomosing system of reverse faults<sup>14</sup> and hence being particularly weak, must have provided the planes of breaking of the crust (Figure 20). This might have resulted in the northward thrusting or popping up of the deeper part and giving rise to the more-than-2500-m high Nilgiri massif. The Anaimalai-Cardamom Hills, further south, must have similarly evolved due to the thrusting up along the P–KSZ.

Strong deformation that the Indian Ocean crust experienced at 0.8 Ma in the Late Pleistocene<sup>80</sup> may possibly be related to the intense fluvial erosion in the northern Sahyadri domain in Maharashtra – to the NNW of the study area – which occurred in the period ranging from late Middle Pleistocene to 0.5 Ma (ref. 81). The Mysore upland in the southern part of the Indian Shield could not have escaped this tectonic event as manifest in the reactivation of ancient faults and the resultant landscape development, including the formation of lakes in the ponded rivers.

1. Naqvi, S. M., Diwakar Rao, V. and Hari Narain, *Precambrian Res.*, 1974, **1**, 345–398.
2. Kailasam, L. N., *Tectonophysics*, 1979, **61**, 243–269.
3. Radhakrishna, B. P., *Curr. Sci.*, 1993, **64**, 787–793.
4. Powar, K. B., *Curr. Sci.*, 1993, **64**, 793–796.
5. Raval, U., in *Continental Crust of Northwestern and Central India* (eds Sinha-Roy, S. and Gupta, K. R.), Geological Society of India, Bangalore, 1995, pp. 37–62.
6. Babu, P. V. L. P., *J. Geol. Soc. India*, 1975, **3**, 349–353.
7. Radhakrishna, B. P., *Bull. Indian Geophysical Union*, 1966, **3**, 95–106.
8. Vaidyanadhan, R., *J. Geol. Soc. India*, 1967, **29**, 373–378.
9. Vaidyanadhan, R., *J. Geol. Soc. India*, 1971, **12**, 14–23.
10. Ramakrishnan, M., in *Geo Karnataka* (eds Ravindra, R. M. and Ranganathan, N.), Karnataka Asst. Geol. Assoc., Bangalore, 1994, pp. 6–35.
11. Rogers, J. J. W. and Mauldin, L. C., in *Volcanism* (ed. Subbarao, K. V.), Wiley Eastern, New Delhi, 1994, pp. 157–171.
12. Harris, N. B. W., Santosh, M. and Taylor, P. N., *J. Geol.*, 1994, **102**, 139–150.
13. Drury, S. A., Harris, N. B., Holt, R. W., Reeves-Smith, G. I. and Wightman, R. T., *J. Geol.*, 1984, **92**, 3–20.
14. Chetty, T. R. K., in *The Archaean and Proterozoic Terrains of Southern India within East Gondwana* (eds Santosh, M. and Yoshida, M.), Gondwana Research Group, Trivandrum, 1996, pp. 77–90.
15. Jayananda, M. and Peucat, J. J., in *The Archaean and Proterozoic Terrains of Southern India within East Gondwana* (eds Santosh, M. and Yoshida, M.), Gondwana Research Group, Trivandrum, 1996, pp. 53–76.
16. Umlauf, D. P., Srikantappa, C. and Kohler, M., in *Proterozoic Geology of Madagascar* (eds Cox, R. and Ashwal, L. D.), Gondwana Research Group, Trivandrum, 1997, pp. 18–19.
17. Srikantappa, C. and Narasimha, K. N. P., *Memoir Geol. Soc. India*, 1988, **11**, 117–124.
18. Naha, K. and Srinivasan, R., *Proc. Indian Acad. Sci. (Earth Planet. Sci.)*, 1996, **105**, 173–189.
19. Rajendran, C. P. and Rajendran, K., *Curr. Sci.*, 1996, **70**, 304–308.
20. Newbold, C., *J. Royal Asiatic Soc. London*, 1846, **8**, 252.
21. Iyengar, R. N., *Earthquake History of India in Medieval Times*, Unpublished Report, Central Building Research Institute, Roorkee, 1999, p. 124.
22. Logan, W., *Malabar* (2 volumes), Asia Educational Services, New Delhi, 1887, p. 759 (1995 Reprint).
23. Paul, J. and 10 others, *Proc. Indian Acad. Sci. (Earth Planet. Sci.)*, 1995, **104**, 131–146.
24. Ramalingeswara Rao, B., *J. Seismology*, 2000, **4**, 247–258.
25. Chaddha, R. K., *Tectonophysics*, 1992, **213**, 367–374.
26. Ramalingeswara Rao, B., *Tectonophysics*, 1992, **201**, 175–185.
27. Gowd, T. N. and Srinivasa Rao, S. V., *J. Geophys. Res.*, 1992, **97**, 11878–11888.
28. Gowd, T. N., Srirama Rao, S. V. and Chary, K. B., *Pageoph*, 1996, **146**, 503–531.
29. Valdiya, K. S., *J. Geol. Soc. India*, 1998, **51**, 139–166.
30. Mandal, P., *Tectonophysics*, 1999, **302**, 159–172.
31. Rastogi, B. K., *Curr. Sci.*, 1992, **62**, 101–108.
32. Rai, S. S., Singh, S. K., Rajagopal Sarma, P. V. S. S., Srinagesh, D., Reddy, K. N. S., Prakasam, K. S. and Satyanarayana, Y., *Proc. Indian Acad. Sci. (Earth Planet. Sci.)*, 1999, **108**, 1–14.
33. Grady, S. A., *J. Geol. Soc. India*, 1971 **12**, 56–62.
34. Drury, S. A. and Holt, R. W., *Tectonophysics*, 1980, **65**, T1–T15.
35. Jayananda, M. and Mahabaleswar, B., *Proc. Indian Acad. Sci. (Earth Planet. Sci.)* 1991, **100**, 31–36.
36. Vasudev, V. N. and Chadwick, B., *Bull. Karnataka Department of Mines and Geology*, 1999.
37. Bouhallier, H., Chardon, D. and Choukroune, P., *Earth Planet. Sci. Lett.*, 1995, **135**, 57–75.
38. Reddy, P. R., Chandrakala, K. and Sridhar, A. R., *J. Geol. Soc. India*, 2000, **55**, 381–386.
39. Radhakrishna, B. P., *J. Geol. Soc. India*, 1964, **5**, 72–83.
40. Senthiaippan, M. and Nair, M. M., in *Geology and Geomorphology of Kerala*, Sp. Pub. No. 5, Geol. Survey of India, Calcutta, 1980, pp. 43–46.
41. Nair, P. K. R., Prasanna Kumar, U. and Mathai, T., *J. Geol. Soc. India*, 1981, **22**, 285–291.
42. Ravindra, B. M. and Krishna Rao, B., *J. Geol. Soc. India*, 1987, **29**, 424–432.
43. Bhat, H. G. and Subrahmanya, K. R., *Intern. J. Remote Sensing* 1993, **14**, 3311–3316.
44. Sreedhara Murthy, T. R. and Raghavan B. R., in *Geo Karnataka* (eds Ravindra, B. M. and Ranganathan, N.), Karnataka Assistant Geologists' Association, Bangalore, 1994, pp. 314–326.
45. Manjunatha, B. R., in *Geo Karnataka* (eds Ravindra, B. M. and Ranganathan, N.), Karnataka Assistant Geologists' Association, Bangalore, 1994, pp. 327–336.
46. Ramasamy, S. M., *Curr. Sci.*, 1995, **69**, 811–814.
47. Ramasamy, S. M. and Balaji, S., *Int. J. Remote Sensing*, 1995, **16**, 2375–2391.
48. Subrahmanya, K. R., *Curr. Sci.*, 1994, **67**, 527–530.
49. Subrahmanya, K. R., *Tectonophysics*, 1996, **262**, 231–241.
50. Benedick, R. and Bilham, R., in *Himalaya and Tibet* (eds Macfarlane, A. et al.), Geological Society of America, Boulder, 1999, pp. 313–321.

51. Balakrishnan, T. S. and Sharma, D. S., *Bull. ONGC*, 1981, **18**, 18–26.
52. Balakrishnan, T. S., *Major Tectonic Elements of the Indian Sub-continent and Contiguous Areas: A Geophysical Review*, Geological Society of India, Bangalore, 1997, p. 155.
53. Chandrasekharam, D., *Phys. Earth Planet Inter.*, 1985, **41**, 186–198.
54. Biswas, S. K., *Tectonophysics*, 1987, **135**, 307–327.
55. Manjunatha, B. R. and Shankar, R., *Marine Geol.*, 1992, **104**, 291–224.
56. Shankar, R. and Manjunatha, B. R., *J. Coastal Res.*, 1997, **13**, 331–340.
57. Ollier, C. D. and Powar, K. B., *Zeit. Geomorph NF*, 1985, **54**, 57–69.
58. Widdowson, W. and Cox, K. G., *Earth Planet. Sci. Lett.*, 1996, **137**, 57–69.
59. Subramanyam, V., Gopala Rao, D., Ramana, M. V., Krishna, K. S., Murthy, G. P. S. and Gangadhara Rao, M., *Tectonophysics*, 1995, **249**, 267–282.
60. Nair, E. V., Kalluraya, V. K. and Hegde, S. V., *GSI Newslett., Marine Wing*, 1997, **13**, 12–13.
61. Holbrook, J. and Schumm, S. A., *Tectonophysics*, 1999, **305**, 287–306.
62. Ouchi, S., *Geol. Soc. Am. Bull.*, 1985, **96**, 504–515.
63. Marple, R. T. and Talwani, P., *Geology*, 1993, **21**, 651–654.
64. Dumont, J. F., *Tectonophysics*, 1993, **222**, 69–78.
65. Kundu, B. and Matan, A., *Curr. Sci.*, 2000, **78**, 1556–1560.
66. Thapliyal, V. and Kulshreshtha, S. M., *Tisglow*, 1993, **4**, 7–17.
67. Valdiya, K. S. and Rajagopalan, G., *Curr. Sci.*, 2000, **78**, 101–105.
68. Valdiya, K. S., Rajagopalan, G., Nanda, A. C., Suresh, G. C. and Upendra T., *J. Geol. Soc. India*, 1999, **55**, 229–237.
69. Raiverman, V., *Sci. Cult.*, 1969, **35**, 29–31.
70. Chadwick, B., in *Geo Karnataka* (eds Ravindra, B. M. and Ranganathan, N.), Karnataka Assistant Geologists' Association, Bangalore, 1994, pp. 81–94.
71. Janardhan, A. S. and Anto, F., in *The Archaean and Proterozoic Terrains of Southern India within East Gondwana* (eds Santosh, M. and Yoshida, M.), Gondwana Research Group, Trivandrum, 1996, pp. 45–195.
72. Parthasaradhi, Y. J. and Vaidyanadhan, R., *J. Geol. Soc. India*, 1974, **15**, 182–188.
73. Demangeot, J., *Finisterra Revista Portuguesa de Geografia*, 1973, **8**, 292–309.
74. Sukumar, R., Ramesh, R., Pant, R. K. and Rajagopalan, G., *Nature*, 1993, **364**, 704–706.
75. Rajagopalan, G. et al., *Curr. Sci.*, 1997, **73**, 60–63.
76. Cartini, C. et al., *Palaeogeogr. Palaeoclimat. Palaeoecol.*, 1994, **109**, 371–384.
77. Nigam, R. and Hashimi, N. H., in *Quaternary Environments and Geoarchaeology of India* (eds Wadia, S. et al.), Geological Society of India, Bangalore, 1995, pp. 380–390.
78. Reddy, P. R. and Vijay Rao, V., *Curr. Sci.*, 1999, **78**, 899–906.
79. Rai, S. S., Srinagesh, D. and Gaur, V. K., *Mem. Geol. Soc. India*, 1993, **25**, 235–263.
80. Krishna, K. S. et al., *J. Geophys. Res.*, 1998, **103**, 17859–17875.
81. Kale, V. S. and Rajaguru, S. N., *Zeit. Geomorph, NF*, 1998, **32**, 311–327.
82. Rajendran, K. and Rajendran, C. P., *Proc. 2nd Ind. Nat. Conf. on Harbours and Ocean Engineering*, CESS, Trivandrum, 1997, pp. 305–314.

ACKNOWLEDGEMENTS. Professor C. N. R. Rao inspired me to look into the aspect of continuing stress build-up beneath the Mysore Plateau in the context of earthquake hazard perception. I am grateful to him and the JNC for the extremely generous support for my work. Dr R. Srinivasan provided a wealth of literature and also great impetus for field work. The author enjoyed the rewarding company of Prof. K. R. Subrahmanya, G. C. Suresh and G. T. Vijayakumar during field work.

I am profoundly grateful to Prof. Pradeep Talwani, Dr R. Srinivasan, Dr C. P. Rajendran and Prof. R. Vaidyanathan for very rigorous and thoughtful reviews of the manuscript. I am grateful to Dr Kusala Rajendran for drawing the diagrams.